Ministry of Higher Education &
Scientific Research
University of Ninevah
College of Electronics Engineering
Communication Department

Investigation of Path Loss

Channel Modeling for 5G

Semaa Kh. Naf'i AL-khero

(B. Sc. in Communication Engineering)

M.Sc. Thesis

In

Communication Engineering

Supervised By

Assist. Prof. Dr. Younis M. Abbosh

Investigation of Path Loss

Channel Modeling for 5G

A Thesis Submitted By

Semaa Kh.Naf'i AL-Khero

(B. Sc. in Communication Engineering)

To

The Council of the College of Electronics Engineering

University of Ninevah

In Partial Fulfillment of the Requirements

For the Degree of Master of Science

In

Communication Engineering

Supervised By

Assist. Prof. Dr. Younis M. Abbosh

2021 A.D   **1442 A.H**

Dedication

To my parents, my brother and sisters who have supported me along the way. I'm very grateful for you.

Supervisor's Certification

I certify that the dissertation entitled (**Investigation of Path Loss Channel Modeling for 5G**) was prepared by **Semaa Khalid Naf'i Al-khero** under my supervision at the Department of Communication Engineering, University of Ninevah, as a partial requirement for the Master of Science Degree in Communication Engineering.

Signature:

Name: Assist.Prof. Dr. Younis M. Abbosh

Department of communication Engineering

Date:

Report of Linguistic Reviewer

I certify that the linguistic reviewer of this dissertation was carried out be me and it is accepted linguistically and in expression.

Signature:

Name:

Date:

Report of the Head of Department

I certify that this dissertation was carried out in the Department of Communication Engineering. I nominate it to be forwarded to discussion.

Signature:

Name: Assist.Prof**.** Dr. Younis M. Abbosh

Date:

Report of the Head of Postgraduate Studies Committee

According to the recommendations presented by the supervisor of this dissertation and the linguistic reviewer, I nominate this dissertation to be forwarded to discussion.

Signature:
Name: Assist.Prof. Dr.Younis M. Abbosh
Date:

Committee Certification

We the examining committee, certify that we have read this dissertation entitled (Investigation of Path Loss of Channel Modeling for 5G) and have examined the postgraduate student (Semaa Khalid Naf'i AL-Khero) in its contents and that in our opinion; it meets the standards of a dissertation for the degree of Master of Science in Communication Engineering.

Signature: Signature:

Name: **Name:**

Head of committee   Member

Date: **Date:**

Signature: Signature:

Name: Name: Assist.Prof. Dr. Younis M. Abbosh

Member   Member and Supervisor

Date: **Date:**

The college council, in it's ………….. Meeting on   , has decided to award the degree of Master of Science in Communication Engineering to the candidate.

Signature: Signature:

Name: Name:

Dean of the College   Council register

Date: **Date:**

Acknowledgments

It has been a wonderful journey here while perusing my Master's thesis. This effort has been a challenge, requiring constant motivation and proactivity. However there were many individuals on my side supporting me. First, I would like to thank Assist.Prof. Dr. Younis Mahmood Abbosh for his guidance and willingness to give me the opportunity to complete the research. He continuously gave good advice and prepared me well through his teaching. I am forever grateful for his patience and the opportunity to be a student of a great engineer. Thank you to all staff of the Department of Communication Engineering specially Dr. Dia Ali and Mr. Mohammed Sameer who have also served as my mentors when I needed them.

Finally, I would like to thank my parents and my friends for their continuous moral support. I would never have made it without any of you.

Abstract

The next generation of cellular communication systems will be faster, more secure, and easier to connect than present wireless networks. To meet the one thousand-fold increase in wireless service demand expected in the next few years, the fifth generation (5G) cellular systems are capable of wireless networks that can be improved in three trends: increasing spectrum usage, improving spatial multiplexing, and increasing bandwidth. The use of wide spectrum is one of the key benefits of 5G. The frequency spectrum below and above 6GHz is among the most researched subjects in the wireless communication systems.

For the design of fifth generation cellular system and analysis of the network coverage, the basic knowledge of channel propagation characteristics especially the path loss of channel parameter in indoor and outdoor environments is important.

In this thesis, the path loss for 5G system has been investigated. Measurements and simulations in the sub- frequency band were carried out at 3.5 GHz in indoor environment at communication engineering department building, Ninevah University, Iraq. It covers one floor of the building including the corridor. Both combination of line of sight (LOS) and non-line of sight (NLOS) channel conditions were taken along the building's second-floor corridor for both practical measurements and simulation using Wireless Insite (WI) software. The 3.5 GHz signal in the LOS condition exhibits less attenuation than the 3.5 GHz signal in the NLOS condition. Both conditions are influenced by neighboring indoor items. Some simulations were also taken in an outdoor environment at different frequencies for comparison between them. For single frequency and multi frequency, path loss for different models was computed after the samples had been taken. For that purpose, the parameters of the path

loss models were computed using MATLAB and Excel software programs. The results show that the path loss exponents were close to the free space value of two for the indoor environment, whereas they are larger than PLEs for the outdoor environment. The standard deviations of the model fits slightly larger than those found for outdoor environments.

List of Contents

List of Figures

VII

List of Tables

List of abbreviations

Abbreviation	Name
3D	Three-Dimension
3G	Third Generation
3GPP	Third-Generation Partnership Project
4G	Four Generation
5G	Fifth Generation
5G-NR	Fifth-generation-New-Radio
ABG	Alpha-Beta-Gama
CI	Close-In free space reference distance
CIF	Close-In with Frequency-weighted
CIR	Channel Impulse Response
DPL	Dual Park lot
DSM	Dual Slope Model
EWLM	Effective Wall Loss Model
FDC	Frequency Dependence Coefficient
FI	Floating-intercept
FSPL	Free Space Path Loss
GEM	Google Earth map
GPS	Global Positioning System
GSM	Global System for mobile communication
ICC-33	International Chamber of Commerce
IEEE 802.11	Institute of Electrical and Electronics Engineers
IOs	Interacting Objects
LAM	Linear Attenuation Model
LOS	Line-of-Sight
LS	Least Square
LTE	Long-Term Evolution
MIMO	Multiple input multiple output
MMSE	Minimum Mean Square Error
mm-W	millimeter Waves
MPCs	Multipath Components
n77	Band number 77
n79	Band number 79
NLOS	Non-Line-of-Sight
NTIA	National Telecommunications and Information Administration
OLOS	Obstruct Line-of-Sight
OPLE	Obstruction Path Loss Exponent
PEC	Perfect Electrical Conductor
PL	Path Loss
PLE	Path Loss Exponent
RF	Radio Frequency
RMSE	Root Mean Square Errors
RSSI	Receive Signal Strength Indication
RT	Ray-Tracing

Rx	Receiver Antenna
SBRT	Shooting – Bouncing Ray Tracing
SF	Shadow Factor
SISO	Signal Input Signal Output
SPL	Single Park lot
SSA	Spectrum Signal Analyzer
SUI	Stanford University Interim
Tx	Transmitter Antenna
UMa	Urban Macro-cellular
UMTS	Universal Mobile Telecommunications System
UWBs	Ultra-Wide Bands
VSG	Vector Signal Generator
WI	Wireless Insite
Wi-Fi	Wireless Fidelity
WINNERII	Wireless world Initiative New Radio II
WLAN	Wireless local area network
WRC	World Radio communication conference
XPD	Cross-Polarization Discrimination

List of symbols

Symbol	Name	Unit
$\emptyset_i$	Azimuth angle	
$\Delta\emptyset$	Phase difference between two waves	
A_r	Effective area of a receiver antenna	
B	Bandwidth	Hz
c	Speed of light	m/s
d	Distance between transmitter and receiver	m
d_0	Reference distance at 1m	m
d_1	Distance from the transmitter to the obstacle	m
d_2	Distance from obstacle to the receiver	m
d_{bp}	Distance of the breakpoint	m
$E\emptyset_i$	Electrical field components of the phi	V/m
EIRP	Effective Isotropic Radiation Power	dBm
F	Noise Figure	
f	Frequency	Hz
h	Height of the obstruction	m
h_{RX}	Receiver height	m
h_{TX}	Transmitter height	m
k	Boltzmann's constant	J/K
l	Direct path length	m
L^{LOS}	Attenuation without any obstacle	dB
L^{NLOS}	Attenuation induced by an obstacle between the transmitter and the recipient	dB
L_p	Path loss	dB
N_p	Number of path	
P_i	Average time of the i_{th} path power	W
P_L	Path loss	dB
P_{L0}	Frequency-dependent reference path loss	dB
P_r	Receiver power	W
r	length of the route mirrored	m
$R_{\parallel}$	Parallel Reflection Coefficient	
$R_{\perp}$	Orthogonal Reflection Coefficient	
$T_{\parallel}$	Parallel Transmission Coefficient	
$T_{\perp}$	Orthogonal Transmission Coefficient	
Te	Equivalent noise temperature of the receiver	K
T_o	Room temperature	K
v	Fresnel parameter	
X_{RX}	Receiver height correction factor	
β	Intersection of the transmitted waveform	
$β_1$	Path loss exponent before the breakpoint distance	
$β_2$	Path loss exponent after the breakpoint distance	
σ	standard deviation	dB
X_{Fc}	Frequency correction factor	

$E\theta$i	Electrical field components of the theta	V/m
G_r	Receiver antenna gain	dBi
G_t	Transmitter antenna gain	dBi
L_s	Loss of cables	dB
N	the power of the thermal noise at the receiver	W
P_t	Transmitter power	W
$X\sigma_{\text{CI}}$	Zero-mean Gaussian random variable	
a	distance attenuation	dB/m
n	Path loss exponent	
α	Floating-Intercept value	dB
β	Line's slope	
γ	Path loss frequency dependence	
η_0	Free impedance of space	Ω
θ_i	Angle of incidence	
θ_t	Angle of transmitted	
ϵ_r	Electrical Permittivity	F/m
θ_i	Elevation angle	
λ	Wavelength	m
φ	Grazing angle	

Chapter One

Background

1.1 Introduction:

In today's world, wireless devices and innovations play an important role, where wireless technologies, from mobile devices and Wi-Fi to automobiles and broadband internet are used by billions of people worldwide [1].

Continued attempts are being made to improve the transmission rate in cellular systems. From second generation (GSM) digital technology having limited data capabilities, cellular mobile radio networks have progressed to third generation (UMTS) systems with wireless data speeds in the range of only few Mbits/s and to fourth generation (LTE) systems with targets of even higher data rates. Relying on several implementations of IEEE 802.11 standards and collectively generally recognized as Wi-Fi. Wireless local area networks (WLANs) have developed through a few megabits per second to hundreds of megabits per second. Although the protocols' ability to handle ever-increasing data rates has improved, the systems' parameters have changed, if anything, to increase the overall connection loss that must be overcome at a given range [2]. Continuously rising demand for higher data rates, higher network capacity, higher energy efficiency and higher mobility has inspired research in the fifth generation of communication systems modeling [3].

In the future, traditional scenarios of the mobile communication system of the fifth generation will affect various parts of life, encompassing home, workplace, entertainment as well as travel, particularly including dense suburban areas, corporations, stadiums,

indoor retail malls, outdoor celebrations, metro, highways and high-speed rail. Fifth generation cellular system incorporates many new device scenarios that have diversified in relation to the 3G/4G scheme as shown in Figure 1.1. The fifth generation includes a variety of novel system architectures with diverse properties such as ultra-high traffic volume, hyper linked density and hyper flexibility. A diversity of techniques, including massive MIMO, millimeter wave (mm-Wave) technologies, ultra-dense networks, and device to device communication, etc. are used to assist end users [4].
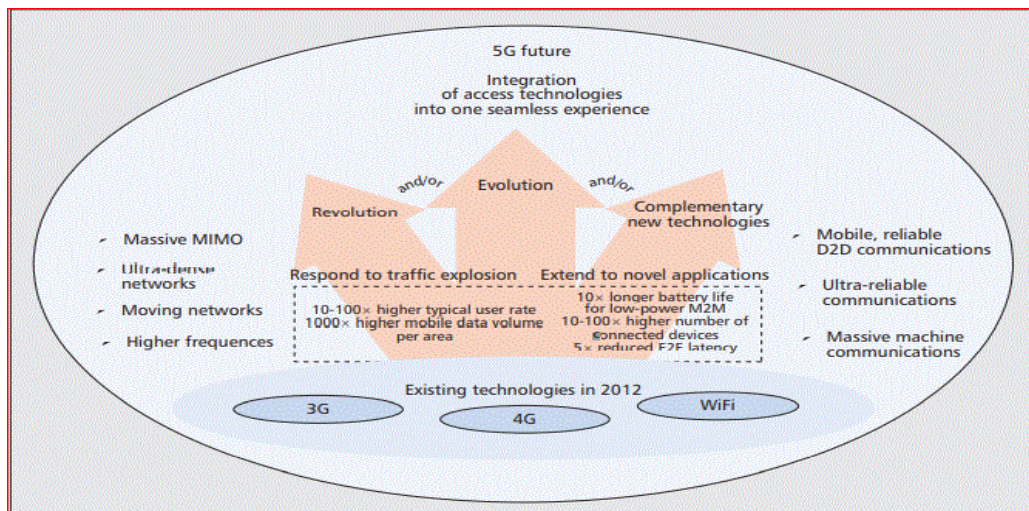
Figure 1.1: Revolution, evolution, and complementary emerging technologies: the 5G roadmap.[5]

Currently, 5G has been the first cellular technology to provide a spectrum band ranging from 400MHz to 90GHz. [6]. The spectrum bands are split into three groups: (low-band, mid-band and high-band) [7]. Mid-bands in 5G-NR include band n77 (3.3-4.2 GHz) and n79 (3.3-4.2 GHz) (4.4-5.0 GHz) [8]. According to United States spectrum allocation chart, the spectrum of 3.3-4.2 GHz is dominated by radiolocation systems, most of which are intended for military and industry purposes. For fixed-satellite communication, the 3.7-4.2 GHz band is often allocated, whereas for military fixed and mobile communication purposes, the 4.4-5.0 GHz

range is assigned [9]. The management of National Telecommunications and Information (NTIA) it has actively proposed that the FCC revise the 3.4-4.2 GHz spectrum allocation to support 5G communication networks by sharing the spectrum between existing operators and 5G telecommunications operators. However, the final radio bandwidth utilized exclusively by 5G systems could be barely within the 3.4-3.7 GHz range[10]. Usually, mid-bands provide a strong combination of 5G networks coverage and capacity: it is important that regulators allocate as much contiguous spectrum as possible in the 3.5 GHz range (3.3 GHz-4.2 GHz). The 2.3 GHz and 2.6 GHz bands should also be approved for 5G use by operators. Current mobile licenses should also be technologically neutral in order to enable 5G networks to grow. In the long term, more spectrums would be required in bands between 3 and 24 GHz to sustain 5G service quality and rising demand. In the 3.5 GHz range, 6 GHz and 10 GHz, which are all part of the WRC-23 phase, this requires more bandwidth[11]. The behavior of electromagnetic waves is somewhat similar to that of existing cellular LTE communication networks using 1-2.5 GHz bands in this frequency range. The penetration, diffraction and reflection capacity of the propagating wave is high below 1 GHz [7]. Bands n258 (24.25-27.5 GHz) and n257 (24.25-27.5 GHz) are typically referred to as mm Wave bands in the 5G-NR standard (26.5-29.5 GHz). For example, the 5G communication networks in the United States, two n258 segments (24.25-24.45 GHz and 24.75-25.25 GHz) and one n257 segment (27.5-28.35 GHz) have been assigned, totaling the bandwidth for this type of bands are 1.55 GHz [12].

The invention of new techniques, as well as the specifications for the fifth generation mobile communication system, has created new issues for wireless channel models. The 5G channel models should accommodate broad scenarios of propagation, including higher frequency

and greater bandwidth, and also a large number of antennas and other factors, while maintaining space, time, frequency, and antenna consistency[4]. Energy-efficient communication requires precise calculation of the connection budget, such that equipment doesn't really waste energy over a certain number of different locations. Existing irregular obstructions and reflectors (chairs, surfaces, shelves...)may generate various reflections, absorption and may be some dispersion in indoor environments. Indoor environments may also differ widely from workplaces to manufacturing plants to laboratories. All these communication scenarios involve precise channel modeling and calculation, as well as outdoor conditions [7].

1.2 Literature review:

Ashok Ch. et al. in 1998 published their investigation of propagation measurements for line of sight and non-line of sight cases at frequencies 900 MHz and 1.89 GHz. This work had been done on three floors of a multi-floor office in tile corridors-cum-institute- cum laboratory building. The research concluded that for non-LOS paths, indoor channel parameters exhibit greater variations. There is no widely accepted indoor channel model and the model of path loss varies from building to building [13].

In 2009, Th. Chrysikos et al. made use of measurements that have been made in the University of Patras at 2.4GHz for diverse indoor propagation topologies, empirical measurement of shadowing deviation can be estimated.

A site-specific validation of indoor RF models was performed based on measurements acquired in a complex indoor propagation environment (the Wireless Telecommunications Laboratory premises) at 2.4 GHz. The shadowing deviation was measured (in dB) based on the losses incurred

by all the different types of walls and floors intervening in the signal direction, It is possible to easily quantify the losses caused by these obstacles with standard equipment for experimentation [14].

In November 2010, Alvaro Valcarce, Student Member and IEEE Antennas and Wireless Propagation Letters published their model of experimental indoor-to-outdoor propagation. In residence indoor-to-outdoor settings, this research presents analytical expressions for modeling path loss and shadow fading. The formulas were calibrated by means of channel power measurements at the radio frequencies of typical cellular systems, therefore ideal for femtocell network channel modeling. The measurements were carried out in the street immediately adjacent to the premises and until distances drop below dBm (10 dB protection margin from the noise floor at dBm) from the outer wall at which the obtained channel power decreases, When the transmitter is in the inner space, which is equivalent to a residential 3G femtocell coverage radius when four users are served, this is around 110 m at 2 GHz [15].

In April 2011.P. Usai, A. Corucci, S. Gligorevic and A. Monorchio, published their investigation about an estimate of an airport surface by a propagation channel, by both simulation and calculation for ray-tracing. The carrier frequency with 120 MHz bandwidth was based at 5.2 GHz. The transmitter was installed at the entrance to the airport terminal, while the receiver was positioned on a van moving around the airport terminal. In terms of path loss, findings were compared for both LOS and NLOS conditions. In terms of the mean of LOS condition, the agreement was very strong for less than 2 dB difference between measurement and ray tracing, whereas in NLOS condition, the power level is transferred around 15-20 m in space with respect to the measured power. A potential explanation for this is inherent GPS tracking error, resulting in a

discontinuity of the GPS coordinate of the receiver, and further resulting in connection error [16].

In 2015, Hang Z., et al. introduced their experimental measurements and empirically based propagation channel models for the frequencies 3.35 GHz, 4.9 GHz and 5.4 GHz in the metropolitan macro cell environment in Xi'an. The measurement at both combinations of channel conditions the line-of-sight (LOS) and non-line-of-sight (NLOS) were included in the calculated situations .Additionally the experimental log-distance path loss for different models are extracted after obtaining the channel impulse response from the measured data. These researchers studied the proposed path loss models by adding the frequency dependency parameter to investigate the relationship between path loss and transmission frequency. They found that in NLOS channel condition, a more exact description of path loss disparities between three frequencies can be produced when FDC is applied [17].

Theodore S. Rappaport et al. in 2015 presented their study on the key parameters for the design of the future fifth generation include the likelihood of line-of-sight (LOS), large-scale path loss and shadow fading models (5G).These measurements have been done at Austin, US for 38GHz and at Aalborg, Denmark for frequencies 2, 10, 18, and 28 GHz. The researchers using the data obtained from propagation measurements to compare alternative of different LOS probability models is carried out for the Aalborg environment, also the path loss models of alpha-beta gamma and close-in reference distance model are examined in detail to demonstrate their value in channel modeling. In addition, omnidirectional path loss models of both single-slope and dual-slope are explored to compare and contrast their root-mean-square errors (RMSE) with calculated path loss values. Based on Aalborg data, the shadow fading

magnitude vs. distance shows a slightly increasing trend in LOS and a decreasing trend in NLOS [18].

In 2016, based on ray tracing data collection, the empirical propagation model for indoor corridor at 5 GHz was proposed by Chi-Hou Chio et al. The model could predict the path loss features of line-of-sight (LOS) and non-line-of-sight (NLOS) for indoor corridor with T-junction using distances from the indoor corridor with T-junction to the transmitter and the receiver, taking into account the width of the corridor. The model has been compared to ray tracing and successful agreements have been seen [19].

In the same year, Shu Sun, Student Member, IEEE et al. published their investigation of prediction accuracy, sensitivity, and parameter stability of large-scale propagation path loss models for 5G wireless communications. This research compares the Alpha-Beta-Gamma (ABG) model, the Close-In (CI) free-space reference distance model and the CI model with a frequency-weighted path loss exponent are all candidates' large-scale propagation path loss models for use throughout the whole microwave and millimeter-wave (mm-W) radio spectrum. These results show that the 1-meter reference distance CI model is good acceptable for outdoor environments, while the CIF model is better suitable for indoor conditions. In current 3GPP models, the CI and CIF models are simple to implement by replacing a floating non-physically based constant with a frequency-dependent constant reflecting loss of free-space path in the Fiirs [20].

Ahmed M. Al-Samman et al. In 2018 presented their experimental measurements based on the propagation characteristics for the frequencies 19, 28 and 38GHz in Kuala Lumpur, Malaysia. Measurements had been done at the University Technology Malaysia

(UTM). These measurements helped the researchers to provide directional five path loss models. For these frequencies, the work provided more detailed information about power delay profile, root mean square delay spread, and azimuth angle spread. For all models shows that the path loss exponent (PLE) and slope line (β) values are less than free space path loss exponent of 2 also for the LOS scenario, the RMS delay spread is low for all bands, and only the guided path is given in some spatial locations [21].

In the same year, H.A. Obeidat, Ramiz Khan et al. published their investigation of the updated model of prediction for indoor path loss. The researchers utilize simulation data and real-time measurements to compare with other indoor path loss prediction models. In the simulation results that among other models, EWLM demonstrates the highest performance as it outperforms the dual slope model twice, which is the second best performance. From the experimental results, comparable observations were reported. Linear attenuation and models with one slope have identical behavior; with the two models parameters of models demonstrate dependence on operating frequency and polarization of antennas [22].

Haider K. Hoomod et al. made use of measurements that have been made in AL-Habebea is an urban area (high-density region) and the second is a rural environment (low-density region) with an operating frequency of 0.8 GHz in the AL-Hindea region. The researchers found that different propagation models were evaluated and compared based on the measured data (Hata Model, ICC-33 Model, Ericson Model and Coast-231 Model). The results of this study and comparison suggest that the Hata model and the Ericsson model display a slight variance from actual urban environment measurements, and that the Hata model usually provides a better rural environment forecast [23].

Maan M. Abdulwahid et al. made a comparison of the C-band and mm-W band performance with distinct frequency ranges. It works for C-band frequencies, 3.5 and 5.2 GHz are included, whereas 38 and 42 GHz for the mm-W band are involved. The researchers used 3D ray tracing simulation for the indoor environment to get the statistical parameters of channel propagation characteristic including delay spread, path loss and received power. The simulation results shown there is a strong connection between the path loss and the distance of separation, where the value of the path loss is much higher than the C-band in mm-W [24].

In 2019, indoor channels path loss modeling and ray-tracing verification for 5/31/90 GHz published by contribution University of South Carolina Columbia, SC, USA. Where the model is built upon a huge number of measurements in indoor environment and simulated through the 3D ray-tracing system. Measurements at each frequency were also made for connection distances up to 50 m in indoor environments and the findings were post-processed in Matlab. To compare results, two types of commonly used log-distance path loss models are used: the reference model of close-in (CI) free-space and the model of floating intercept (FI). These measurements helped the researchers to provide a comparative path loss simulation with measurements for various frequencies, antennas and channel conditions. Findings was showed that CI model slopes vary by less than 0.3 between ray-tracing and measurements, and standard model deviations vary by less than 2 dB for all line of sight (LOS) case frequencies; differences are less than 0.6 for slope and 5 dB for standard deviations for a non-light-of-sight (NLOS) channel condition, demonstrating the usefulness of ray-tracing for these frequencies and settings [25].

In the same year, Mohammed S. Salim, Khalil H. Sayidmarie et al. introduced their experimental measurements and simulations to study the transmission of radio waves. The measurements had been done at the University of Mosul, Iraq. The researchers used simulations and measurements at different locations, directions, and heights of the Tx and Rx antennas to estimate the power obtained from a WLAN access point operating at 2.45 GHz. These measurements helped the researchers to provide a comparative of the two scenarios. The results of the path loss models show that in this indoor environment, the path loss exponent (PLE) is less than the of free space path loss exponent (n=2) for the LOS scenario. On the contrary, PLE is larger than free space path exponent for the OLOS scenario. This indicating that when there is no direct path between the transmitter and receiver, the path loss increases [26].

Ferrous Hossain et al. they carried out an effective study of indoor radio wave propagation using 4.5 GHz frequency band was implemented. The researchers have been used proposed three-dimensional (3-D) ray-tracing (RT) for the modeling and measurements. On the outcomes of the measurement, several comparisons were made: The proposed method, and the actual simulation of the SBRT method with regard to obtained signal strength indication (RSSI) and path loss indication (PL). The comparative results indicate that the RSSI and the PL of the proposed RT have better measurement agreements than the traditional SBRT outputs [27].

In 2020, M. Schmieder et al. published their investigation about wideband channel measurement campaign in an industrial setting for frequencies 3.7 and 28 GHz. The researchers used CIR snapshots for power delay profiles were analyzed showing that there are few specular multipath components in the radio channel and are filled with dense

multipath components with a delay of up to 600 ns. A frequency-dependent model of ABG path loss was fitted using the outcomes for LOS and NLOS conditions; at 3.7 and 28 GHz comparison with other papers' recent findings and the novel 3GPP TR 38.901 the indoor factory model shows that the characteristics of path loss are special and highly scenario-dependent [28].

Y. Guan et al. in the same year of 2020, introduced their Industrial measurement based on comparative analysis of channel characterization, i.e. path loss and Ricean K-factor at 4.9 and 28GHz. The outcomes of comparative channel measurements in indoor factory environments, discover that with frequency, the PLE increases in both LOS and NLOS situations , at 4.9 GHz (1.9 in LOS and 2.2 in NLOS) compared to the 28 GHz (2.2 in LOS and 2.6 in NLOS). In LOS situations, the higher PLE is observed in indoor factory environments and the smaller PLE with both 4.9 GHz and 28 GHz in NLOS situations. In addition, in this paper, the effect of antenna height on the propagation channel is studied. The researchers found that with the increasing antenna height in LOS and NLOS conditions, the PLE decreases [29].

1.3 Thesis Aims:

This thesis aims at focusing on the path loss of the channel characterizations for the fifth generation (5G) cellular system. Evaluate simulation results with path loss models results from a set of measurements. These measurements were performed using vector signal generator (VSG), signal spectrum analyzer (SSA), additionally specific computer simulations using Wireless InSite and processing the data using Matlab and Excel software. In this thesis, simulations and measurements focus on one frequency band which is 3.5 GHz in C band with single-input single-output (SISO) channel

for indoor environment, also comparing between two frequency bands below and above 6GHz with two types of antennas using Wireless InSite software for outdoor environment. In simulations we're capable of quantify the channel's path loss. In this thesis, it can be focused on study of path loss in different channel scenarios in indoor and outdoor environments. Comparison of simulations with measurements for a narrow band signal is also included.

1.4 Thesis Layout:

In this segment, an overview of the thesis is provided:

1. Chapter one describes the importance of the fifth generation and gives an overview about the work and efforts that have been made within the research field of 5G and channel characterization and ultimately indicates the aim of the thesis.

2. Chapter two includes explanation distinctive sort of path loss models and how different factors contributing and effecting the received energy of the signal.

3. Chapter three presents a brief description of the experimental and simulation setup, equipment's utilized in the measurement and the way the test was performed, moreover the specifications in computer simulation Wirless InSite software.

4. Chapter four includes results and discussion of measurement and simulation study for different channel types. Path loss is compared in indoor corridor channels of simulation to that measurement for 3.5GHz.

5. Chapter five presents comparison between simulation results and three types of path loss models results for both types of antennas in outdoor environment.

6. Chapter six contains conclusions of the whole thesis and some suggestions are given for future work.

Chapter Two

Principles and Models

of Propagation

2.1 Introduction:

The waves pass from transmitting antenna to a receiving antenna via the so-called channel [30]. The channel plays an important role in device efficiency and is an integral part of developing and implementing wireless communication systems[31]. There are a variety of methods for measuring the performance of any wireless communication channel, and this performance varies from one network to the next due to the network's design and the devices utilized in it [30].

Path loss is the fundamental quantity that characterizes the wireless transmission channel and affects the efficiency of any communication device. It's the opposite of the path gain, which is the sum of signal power obtained. In the narrow band system, it is defined as the amount of decay in the received power at a certain stage (carrier) frequency. It can be extracted from the power of the multi path components (MPCs) for the narrow-band and the ultra-wide band (UWB) systems, which involves the combined effects of attenuation and time dispersion [32]. Modeling of several physical mechanisms (free-space attenuation, vegetation and attenuation by reflection, attenuation by diffraction, building penetration loss, etc.) is used to describe how radio waves propagate. This modeling is required for the design of telecommunication systems as well as their actual field deployment once they have been designed [33].

The fundamental mechanics and concepts of electromagnetic signal transmission and measurement are discussed in this chapter. Reflection,

scattering, diffraction, refraction and multi path are these physical concepts. In addition, several of the basic propagation models that have been recently defined and widely utilized construct wireless communications will be reviewed in this chapter.

2.2 Principles and Propagation Mechanisms

2.2.1 Reflection:

When an electromagnetic wave passes from a medium or water towards another medium, the signal can be guided in a various direction at the interface[26]. In wireless communications, whenever the media or substance intercepted by the wave is substantially large in comparison to the signal wavelength, it is often referred to as reflection as shown in Figure2.1[34]. The degree whereby the signal is reflected depends on the frequency, electrical conductivity (or refractive index), the penetration and resistivity of the two medium, and the electromagnetic signal incidence angle.

From Fresnel plane wave reflection coefficients and Transmission coefficients are computed as follow equations [35]:

$$R_\perp = \frac{\cos(\theta i) - \sqrt{\epsilon r}\,\cos(\theta t)}{\cos(\theta i) + \sqrt{\epsilon r}\,\cos(\theta t)} \qquad (2.1)$$

$$R_\parallel = \frac{\sqrt{\epsilon r}\,\cos(\theta i) - \cos(\theta t)}{\sqrt{\epsilon r}\,\cos(\theta i) + \cos(\theta t)} \qquad (2.2)$$

$$T_\perp = \frac{2\cos(\theta i)}{\cos(\theta i) + \sqrt{\epsilon r}\cos(\theta t)} \qquad (2.3)$$

$$T_\| = \frac{2\cos(\theta i)}{\sqrt{\epsilon r}\,\cos(\theta i) + \cos(\theta t)} \qquad\qquad (2.4)$$
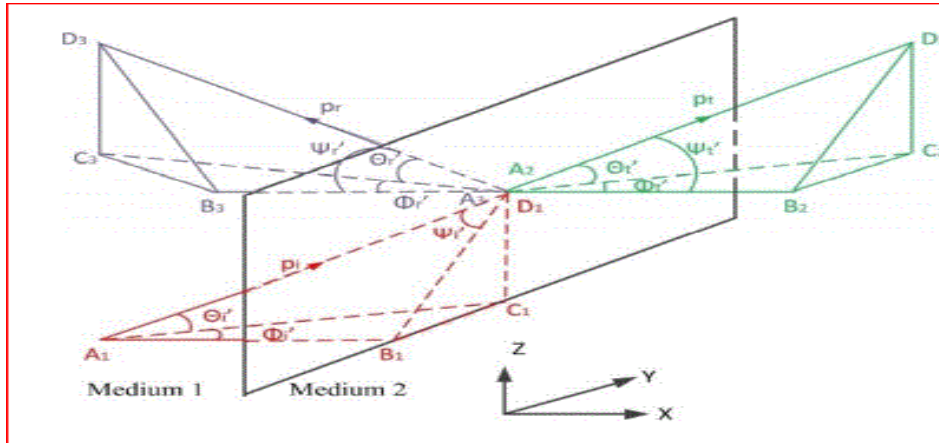
Figure 2.1: Reflection and transmission by plane interface at the oblique wave incidence. [36]

2.2.2 Refraction:

The phenomenon that happens when electromagnetic wave will pass between two medium with different conductivity or a material with a continually varying dielectric permittivity through an interface, is called refraction[37]. The direction wherein the signal propagates through as with reflection, as well as the percentage of the wave power that propagates through the medium or along the interface are all influenced by the signal's electrical and magnetic properties. It is also affected by the electromagnetic wave frequency [38].

2.2.3 Diffraction:

The continuation of radiating waves from optically lit to darkened parts of a barrier is referred to as diffraction[39]. The wall corners in a corridor, rectangular pillars and stair cases are an example of materials that could cause diffraction as shown in Figures 2.2 and 2.3. Nonetheless,

the field intensity decreases significantly in the intercepted area, but the diffraction field typically has sufficient strength to generate significant received signal [32].

The definition of the perfectly absorbing knife edge contains one theoretical mathematical model used to gain better understanding of the diffraction process.
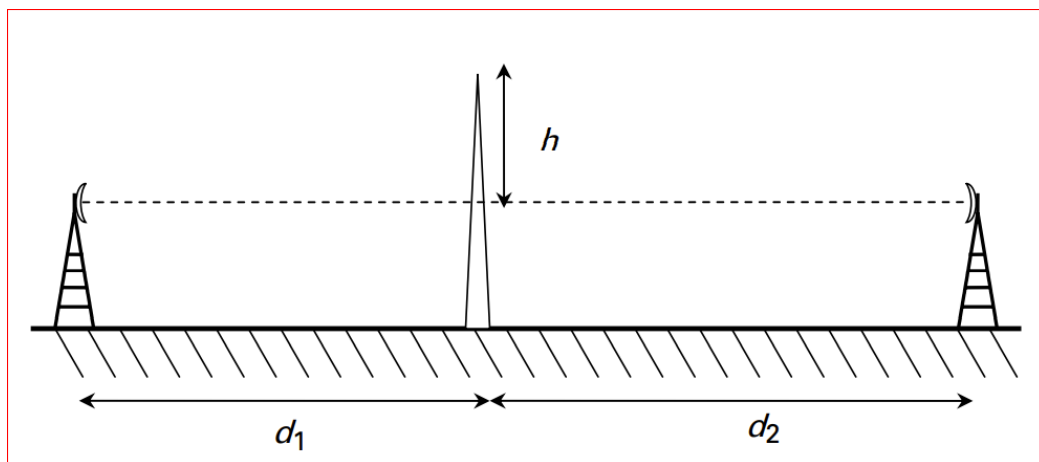
Figure 2.2: The direction geometry for diffraction of the knife-edge.[35]
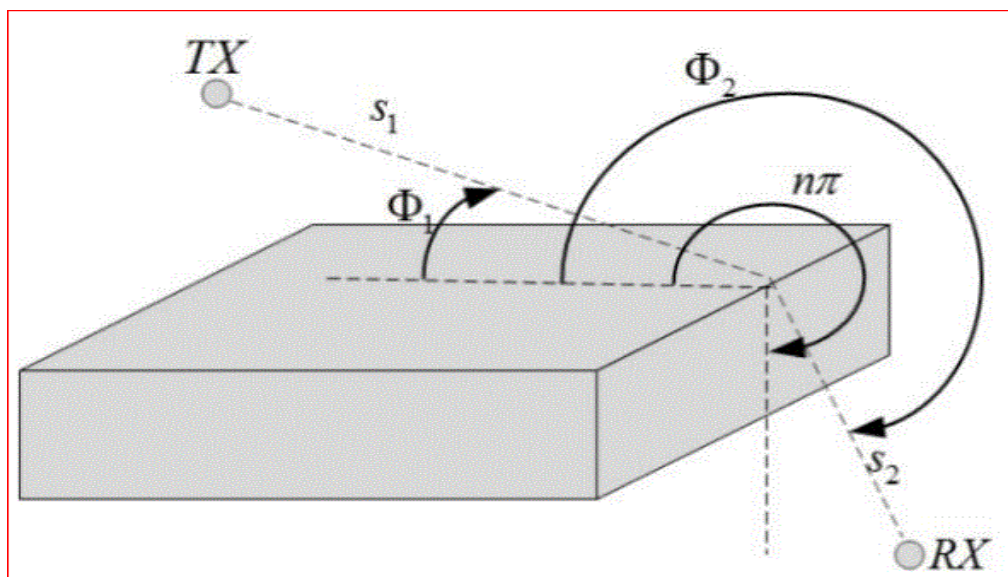
Figure 2.3: Geometry for wedge diffraction coefficients.[36]

The proportion of signal strengths without and with the barrier is referred to as the loss of diffraction. The diffraction loss is impacted by the geometry of the path and the frequency of operation. All the related variables can be absorbed into one single parameter: the Fresnel parameter. As shown in Figure 2.2 the Fresnel parameter v is given by equation (2.5).

$$v = h * \sqrt{(\frac{2}{\lambda} (\frac{1}{d1} + \frac{1}{d2})}) \qquad (2.5)$$

The loss of diffraction is then a function of the parameter Fresnel. The method of calculating the diffraction loss is very complex, including the summation of sequences, from the Fresnel parameter [35].

$$\text{Loss} = 6.9 + 20\log (\sqrt{(v - 0.1)^2 + 1} + v - 0.1) \text{ dB} \qquad (2.6)$$

2.2.4 Scattering:

This physical situation happens whenever the wavelength of the signal of the incident is close, equal to, or greater size as the object it makes contact which it, as shown in Figure 2.4 [40].In a wireless communication model, the actual received signal is also stronger than that predicted by models of reflection and diffraction. This is because the reflected energy is distributed in all directions due to dispersion when a radio wave reaches a rough surface [34]. The frequency of 3.5 and 28 GHz used in this thesis. These frequencies are in the centimeter wave region of the electromagnetic spectrum. This relation between an electromagnetic signal's frequency f and wavelength λ is given by c = λf, whereby c is equals to 3 x 10^8 meters/second (light speed). For 3.5 and 28GHz, these produce free-space wavelengths of 21cm and 10cm respectively. Most of the physical effects observed throughout

transmission are probably to be reflections rather than dispersion, due to the short wavelength. Scattering, however, is still possible and still must be considered. Multiple copies of the transmitted signal will normally enter the receiver due to this potential scattering and reflection. They can intervene constructively or destructively. Constructive interference occurs if one signal's peaks and troughs coincide with those of another signal. Destructive interference occurs when one wave's peaks and troughs appear to cancel another wave (often called multipath or small-scale fading).
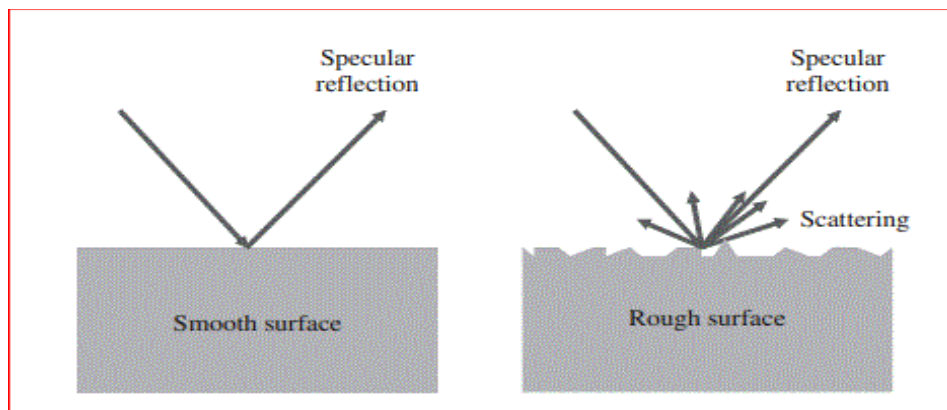
Figure 2.4: Scattering by a rough and smooth surfaces. [41]

2.2.5 Multipath Propagation

The radio channel between the transmitter TX and the receiver RX acts as the transmitting medium for wireless communications. There are a variety of different propagation routes that can get the signal from the TX to the RX. A Line Of Sight (LOS) link between TX and RX may exist in some cases. In addition, the signal will reach from the TX to the RX by reflecting or diffracting by various Interacting Objects (IOs) in the environment, buildings, mountains (for outdoor environments), windows, walls, etc. (for indoor environment). There are several different propagation directions that can be taken. Every path has its own amplitude, delay (signal runtime), direction of departure from the TX, and

direction of arrival, as shown in Figure 2.5; more specifically, the components have different phase shifts with respect to one another [33].
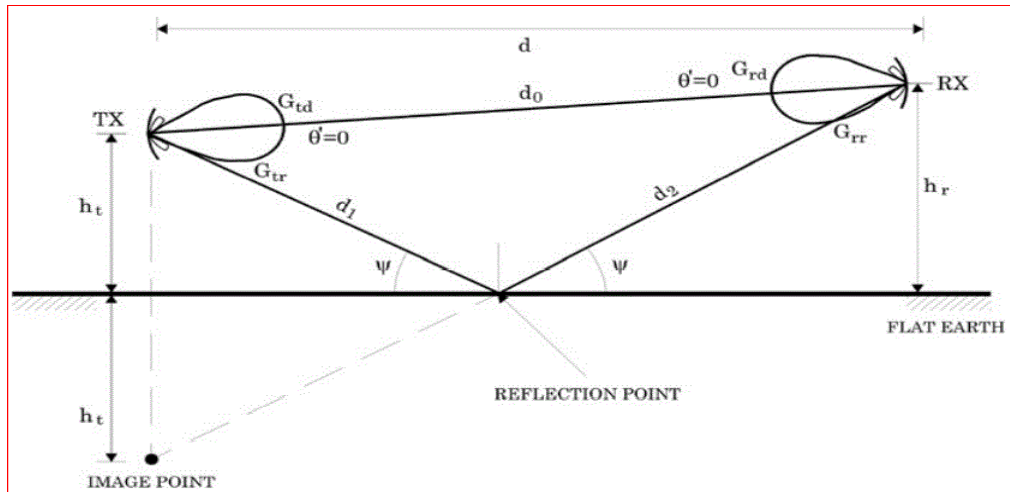
Figure 2.5: Simple geometrical definition of receipt of multipath. [41]

2.2.6 Receiver Noise and Noise Figure:

A receiver's sensitivity or threshold is an important attribute which defines the efficiency of a cellular communication connection. The threshold is the minimum signal intensity required for a specific output. The generally dominant aspect of noise at the receiver is caused by thermal disruptions of electrons. This disruption is correlated with Brownian motion. A Gaussian amplitude distribution is the basic model for this noise. It is spectrally "white," meaning for all wavelengths; its power spectral density is constant. For the whole frequency spectrum, noisy does indeed have a power spectral density usually represented $N_o/2$. This thermal noise, in probabilistic terms, is also irrespective of the wireless signal obtained. The thermal noise is additive to the receiver's noise. Usually, this thermal noise is commonly referred as Gaussian white additive noise (AWGN) [37].

Theoretically, the power of thermal noise in the receiver can be calculated as follows.

$$N = kT_0B \qquad (2.7)$$

While, N is the power of the thermal noise at the receiver, in watts, k is Boltzmann's constant $= 1.38 \times 10\text{-}23$ J/K, T_o is the standard noise or room temperature which is typically given as 290 K and B is bandwidth of the receiver in Hz . In reality, this thermal noise power at the receiver adds noise to various components present. This makes the real noise higher than that only expected by (2.7). Amplifiers, filters, wires, etc. are elements that make up the receiver. As a result, the most reliable method for determining thermal noise power is to characterize it using an effective temperature or noise figure. As a result, a more realistic equation for calculating thermal noise power is as follows:

$$N = kT_0 \mathrm{B}F \tag{2.8}$$

Where, $F = (1 + \frac{Te}{T0})$ is Noise figure of the receiving device (dimensionless) and T_e is the equivalent noise temperature of the receiver in K. When estimating a connection budget, considering the noise at the receiver is more important. Effective in measuring the noise in decibels at the receiver (dB). The equation that measures the receiver's real noise power in decibels relative to a particular power level (in this case dBm, or dB relative to 1 mW) is given as following equation.

$$N\,(dBm) = -174\,dBm/Hz + 10\,\log\,(B) + F_{\mathrm{dB}} \tag{2.9}$$

The constant theoretical value of the power spectral density in dBm/Hz for T=290 K is the -174 factor [43].

2.3 Propagation Modeling:

The purpose of the propagation modeling is to define the likelihood that the cellular communication system's efficiency meets standards and provides high service quality [40]. The path loss model is a popular model for illustrating the effects of the surrounding environment on the channel. It investigates the fading behavior (power attenuation factor) as a function of distance and frequency [38]. The reliability and applicability

of the path loss model will influence the cost and efficiency of the network. In terms of communication network architecture, the main objective of wireless channel modeling is to estimate the signal intensity obtained over a range of link distances. In order to prevent or compensate for distortion, wideband channel models are often used to predict parameters that are useful in design system. The signal strength obtained can be estimated whereas if the quantities of attenuation and transmission strength are known. The path loss is only the dB variation among both the transmitted signal power and received signal power (or whether the transmission-to-receive power ratio is in linear units).

Due to all phenomena such as reflections, scattering, diffraction, and spatial spreading, path loss will "encapsulate" signal intensity reduction. Path loss often is frequently influenced by the type of setting, frequency, and height of the antenna. Urban, rural, and suburban are different types of environments. Businesses start the design process by selecting the model that best suits the scenario, based on the implementation of the communication system and the variables previously provide [40].

2.3.1 Free Space Path loss Model:

There is no barrier between the transmitter and receiver antenna in the model of free space path loss and a direct line of sight (LOS) path between them is open. Satellite communication and microwave line of sight radio links is the common scenario for the LOS communication. As for the other large-scale fading model, the obtained power decreases with the increased distance. Energy conservation demands that the power density integral of any closed surface surrounding the transmit antenna must be equal to the power transmitted [41].From the Friis free space equation the received power relationship is given as equation (2.10).

$$P_r\left(d\right) = P_tG_tA_r * \frac{1}{4\pi d^2} \tag{2.10}$$

Here P_r is the receiver power, P_t is the transmitter power, G_t is the transmitter antenna gain, A_r refers to the effective area of a receiver antenna and d is the distance between transmitter and receiver. The effective area is now related to the receiver antenna gain G_r .The one that can be written.

$$G_r = 4\pi * \frac{Ar}{\lambda^2} \tag{2.11}$$

From equation (2.10) and (2.11) it can be deduced that:

$$P_r(d) = P_t G_t G_r \frac{\lambda^2}{(4\pi d)^2} \tag{2.12}$$

So if the antennas have a unity gain then the path loss equations become,

$$L_P = \frac{(4\pi d)^2}{\lambda^2} \tag{2.13}$$

Now in logarithmic scale Path loss,

$$L_P(dB) = 20\log\left(\frac{4\pi d}{\lambda}\right) \tag{2.14}$$

As, $\lambda = \frac{c}{f}$, where f is the frequency of the system. Now for centimeter wave the equation becomes as follow [44].

$$L_P(dB) = 20\log\left(\frac{4\pi d\, f \times 10^9}{c}\right) \tag{2.15}$$

$\blacktriangleright$ $Lp(dB) = 20log(\frac{4\pi d\, f \times 10^9}{3 \times 10^8})$

$\blacktriangleright$ $Lp(dB) = 20\log\left(\frac{4\pi}{3}\right) + 20\log f + 20\log d$

$\blacktriangleright$ $Lp(dB) = 32.44 + 20\log f + 20\log d \tag{2.16}$

2.3.2 Close-In Path Loss Model

Close-in (CI) free space reference distance path loss model system is one of the most common path loss model systems. The CI model can be used for frequencies above or below 6 GHz. It is given under the CI model in equation (2.17).

$$PL_{CI}(f_c, d)[dB] = FSPL(f_c, d_0)[dB] + 10nlog_{10}(d/d_0) + X\sigma \qquad (2.17)$$

$$\text{For, } d > d_0, \text{ where } d_0 = 1\ m.$$

Where, the separation between transmitter and receiver is referred as d, n is the path loss exponent and $X\sigma$ refers to the Gaussian random variable shadow fading with zero mean and standard deviation σ in dB [45]. *FSPL* refer to the free space path loss for Friis (FSPL) [46].

FSPL for the frequency spectrum of GHz now,

$$FSPL(f_c, d_0)[dB] = 20log_{10} \times (\frac{4\pi fc\ d0 \times 10^9}{c}) \qquad (2.18)$$

Now here, the speed of light is c. it can be now simplify the equation by considering d_0 = 1m.

The equation is standardized by giving d_0=1m value and becomes universal and very precise in model prediction. Now it becomes the equation

$$FSPL(f_c, d_0)[dB] = 32.44 + 20log_{10}f_c \qquad (2.19)$$

So, it is now possible to write (2.19) as [45]

$$PL_{CI}(fc, d)[dB] = 32.44 + 20log_{10}f_c + 10nlog_{10}d + X\sigma \qquad (2.20)$$

$$\text{where } d \geq 1\text{m}$$

Another attenuation factor is to be adding in the case of cross polarization.

The best result for antenna cross polarization cases is the cross-polarization discrimination (XPD) factor with the CI path loss model [45]. The attenuation and cross-polarization discrimination (XPD) parameter is close to the loss per floor or wall loss [47]. XPD factor best matches the calculated data through an MMSE (minimum mean square error) method [45].

PL (f_c, d) $[dB]$ = FSPL $(f_{c,} d_0)$ $[dB]$ + $10nlog_{10}d$ + X_σ CIX +XPD (2.21)

Another kind of CI model supplement is when various kinds of obstacles are put between the transmitter and the receiver. To obtain the new device value, it can add an attenuation factor known as the obstruction path loss exponent (OPLE) to the current CI model. Therefore, the equation becomes [47].

PL$_{CI}$ (f_c, d) $[dB]$ = FSPL $(f_c,$ d$_0)$ $[dB]$ + $10nlog_{10}d$ + X_σ + $OPEL$ (2.22)

The value of OPEL is based on the model COST-231Motley-Keenan. OPEL for the same distance (d=1m) can now be determined as

$OPEL = L_{meas}{}^{LOS} (d1m) + L_{meaas}{}^{NLOS} (d1m) [dB]$ (2.23)

Here, L ^{LOS} is for attenuation without any obstacle or wall occurring. The attenuation induced by an obstacle between the transmitter and the recipient is referred to as L ^{NLOS} [47].

2.3.3 Floating-Intercept Path Loss Model

The floating-intercept (FI) path loss model is another alternative for the path loss model. For the WINNERII Project and 3GPP channel models, it is one of the propagation models implemented in channel

standardizations [48].This model is also defined as the model of the alphabet. It is possible to convey the FI design as

$$PL_{FI}[dB] = \alpha + 10.\beta log_{10}(d) + X\sigma \qquad (2.24)$$

α refers to the intercept value in dB. β refers to the line's slope that characterizes the dependency of the distance of loss. $X\sigma$ refers to the Gaussian random variable shadow fading with zero mean and standard deviation σ in dB [49]. β only functions as a basic slope that provides the best fit for a data scatter plot and in any way has no physical basis or frequency dependence and β has no physical basis or frequency dependence whatsoever. Furthermore,$\alpha$is set equal to the reference distance of free space near the antenna [50]. In logarithmic units, $X\sigma$ is a zero mean Gaussian random variable with standard deviation σ, which defines the large-scale signal fluctuations of the mean distance path loss, also known as the shadow factor in the literature (SF). The FI model has a mathematical curve fitting approach without any physical anchor over the calculated path loss range [45]. Similar to the CI model, X_{σ} is the shadow fading log-normal random variable [41]. For both LOS and NLOS conditions, both the close-in free space reference distance (CI) model and the floating intercept (FI) model can be used to specify 5G wireless channel propagation [50].

2.3.4 Dual Slope Model (DSM)

The model of single-slope path loss normally fails dependence on the physical environment in dense and millimeter wave capable networks to consider the PLE (path loss exponent). Such limitations result in the consideration of the model of dual slope path loss [51]. The relation distance does not offer the best fit and the model of loss of dual-slope path with a distance break-point is given in the following equation [52].

$$\text{PL}_{\text{LDS}} [dB] = \{ PL_0 + 10\beta 1 \, log10d + X\sigma$$

$$d \leq d_{bp}$$

$$PL_0 + 10\beta_1 \, log10d_{bp} + 10\beta_2 \, log10 \, \frac{d}{d_{bp}} + X\sigma, \hspace{2cm} (2.25)$$

$$d > d_{bp}\}$$

d_{bp} here is the distance of the breakpoint, P_{L0} is referred to as a path loss model for 1m reference distance, The path loss exponent (PLE) before and after the breakpoint distance is expressed by β_1 and β_2, d is the distance from the transmitter to the recipient and $X\sigma$ is a Gaussian-distributed shadow fading with a zero mean [53]. A default constant or a joint frequency and height based value may be used as the break-point distance for convenience [52].

2.3.5 Linear Attenuation Model (LAM)

Authors suggested another method in 1991, tests were carried out on frequency ranges (0.85, 1.9, 4 and 5.8 GHz), it was concluded that total loss L is the amount of free space loss L_{FS} and loss factor in the frequency and building range (0.3 to 0.6 dB/m). It is given in the following equation [22].

$$PL \, (dB) = P_{L0} \, (dB) - 20n \, log_{10} \, (d) - a \cdot d \hspace{2cm} (2.26)$$

Where PL dB is the mean path loss (dB), P_{L0} dB is the frequency-dependent reference path loss (path loss at 1 m distance from the transmitter), n is the of path loss exponent that expresses the rate of loss of attenuation, a refer to the distance attenuation (dB/m) and d indicates the distance in meters. When the average power values obtained are determined experimentally (in dBm) over selected locations of a given propagation topology, and the total EIRP is known (in dBm), the

attenuation over distance (in dB/m) is estimated by the distance attenuation (in dB/m).The formula is:

$$a= \frac{EIRP\ (dBm)-Pr(dBm)-10nlog10(d)-43.33dB}{d} \qquad (2.27)$$

Where the reference path loss (path loss 1m away from the transmitter) is 43.33 dB, for the frequency is 3.5 GHz [54].

2.3.6 Stanford University Interim (SUI) Model

One of the suggested models for frequency ranges below 11 GHz is the Stanford University Interim (SUI) model developed by Stanford University. The SUI model for IEEE 802.16e systems can be used to measure 3G and 4G cellular networks operating above 2 GHz in the microwave bands [55]. The model contains three of the most common terrain categories. The IEEE 802.16 broadband wireless communication working group proposes this model [56]. The SUI models are split into three terrain groups, namely A, B, and C. Form A is correlated with maximum path loss and is suitable for hilly terrain with moderate to heavy densities of vegetation. Minimum path loss is correlated with Form C and refers to flat terrain with light tree densities. Form B is characterized by mainly flat terrain with intermediate terrain, small tree densities to high tree densities or hilly terrain below is the regular SUI design [57].

$$PL_{SUI}\ (d)\ [dB] = FSPL\ (f,\ 1m)\ [dB] + 10nlog_{10}\ d\ /1m + X_{fc} + X_{RX} + X_{\sigma}$$
(2.28)

Where it is possible to obtain FSPL from equation (2.19)

$$n = a - b.\ h\ (m) + \frac{c}{h}\ (m) \qquad (2.29)$$

$$X_{fc} = 6. \, log_{10} \, (f_{MHz} \, /2000), \, f > 2 \, GHz \hspace{2cm} (2.30)$$

For types A and B of terrain,

$$X_{RX} = -10.8 * log_{10} \, (\frac{h \, (m)}{2}) \hspace{2cm} (2.31)$$

And for C type terrain,

$$X_{RX} = -20 * log10 \, (\frac{h \, (m)}{2}) \hspace{2cm} (2.32)$$

$X\sigma$ is a zero mean Gaussian random variable, with standard deviation σ, in logarithmic units, ranging from 8.2 dB to 10.6 dB [39]. X_{Fc} is the frequency correction factor, X_{RX} is the receiver height correction factor, the transmitter height is also indicated by h_{TX} and the receiver height of the antenna is indicated by h_{RX} in meters [55]. In all three settings, namely rural suburban and urban, the SUI model is used to predict the path loss [58].

2.3.7 Alpha-Beta-Gama Model

ABG is a large-scale model of multi-frequency path loss [59]. It's a model focused on frequency and distance. This model can be written as:

$$PL^{ABG} \, (d) \, [dB] = 10\alpha log_{10} \, d/ \, d_0 + \beta + 10\gamma log_{10} \, (f/1GHz) + x_{\sigma ABG} \hspace{0.5cm} (2.33)$$

$$For, \, d \leq d_0, \, d_0 = 1m$$

In order to minimize the error between the model and the measured data, the three model parameters α, β and γ are calculated by finding the best fit values [60]. In terms of frequency and distance, PL^{ABG} refers to the path loss in dB, α shows the path loss slope with the log distance, β is the dB floating offset value, an optimized offset parameter. γ models the path loss frequency dependence, where f is in GHz. The distance and frequency are defined by α and γ coefficients. Dependence on path loss and ultimately $X\sigma$ ABG stands for zero Gaussian mean random variable

with σ standard deviation (SD) in dB [61]. In addition, α, β, and γ are optimized from closed-form solutions that reduce the normal SF (shadow fading) deviation [59]. Via MMSE, the ABG model is resolved to minimize σ by simultaneously solving for α, β, and γ [45].

2.3.8 Two ray model ground reflection path loss model

A two-ray model is the simplest type of ray tracing, where the obtained signal has an earth-reflected wave presence [62]. Signal-based modeling methods of propagation are necessary because physical process such as reflections, scattering, diffraction and other phenomena generated by artifacts in the environment impact signal attenuation. Whenever the communication link area becomes more crowded with objects or people, the free space model is not good enough to estimate the received signal [53]. Multipath models perform path loss calculations depend on geometrical pathways taken by the signal from the transmitter antenna to the receiver antenna. The two-ray model is shown in Figure 2.6, in which, both line of sight and straight line paths reflected from the earth, walls as well as other objects may have these geometric paths. The two-ray model is a simple multipath model. This type of model is utilized for any communication link requiring the use of a near-earth transmitter and receiver with minimum obstacles. The reflected ground signal at the receiver end may either intervene constructively or destructively.

The total strength obtained can be written as equation (2.34).

$$P_R = P_T G \left(\frac{\lambda}{4\pi}\right)^2 \times \left\{\frac{1}{d} + (\Psi)\, e^{-j\Delta\phi} /^r\right\}^2 \tag{2.34}$$

Here, P_R refers to the received power strength, P_T refers to the power intensity transmitted, G refers to the antenna gain, λ refers to the wavelength of the operating frequency of the transmitter, d refers to the direct length between the transmitter and the receiver that corresponds to

the Fresnel reflection coefficient, which represents the obstacles, φ is referred to as gazing angle, the direct path length is l, r refers to the length of the route mirrored and the phase difference between two waves is assigned to $\Delta\emptyset$. It is possible to express the phase difference as [63]:

$$\Delta\emptyset = \frac{2(r-l)}{\lambda} \qquad (2.35)$$

The path loss can be determined from the formula below after obtaining the obtained power.

$$PL\,[dB] = 10log_{10}\left(\frac{P_T}{P_R}\right) \qquad (2.36)$$

The two-ray model path loss thus becomes,

$$PL_{2ray} = -20log_{10}\left[\left(\frac{\lambda}{4\pi d}\right)^2 + (\Psi)^{-j\Delta\emptyset}\right] \qquad (2.37)$$

If we assume that the angle of incidence with the ground is similar to grazing, which means that the magnitude and phase of the reflection coefficient will be close to one and 180 respectively, it is then possible to write a 2-ray model as [49].

$$PL_{2ray} = -20log_{10}\left[\left(\frac{\lambda}{4\pi d}\right)\left\{2\sin\left(\frac{2\pi h_t h_r}{\lambda d}\right)\right\}\right] \qquad (2.38)$$

Here, respectively, h_t and h_r refer to the transmitter and receiver heights.

The two-ray model can be generalized to four-ray, six-ray, and ten-ray models in which the difference in the path between each reflected ray is determined by the image process [62]. The two ray model like all models has certain flaws. The first vulnerability would be that it assumptions the ground is absolutely perfectly level. Scattering, reflection, and even diffraction effects may be caused by sharp edges or irregularities on the ground. A second drawback is that barriers are

possibly in a realistic application or device, so this model is only helpful in areas where there are no nearby obstacles in the transmitter and receiver line of sight path. The approximate model also assumes that for the LOS path and the reflection the antenna gains (at both Tx and Rx) are same. This approximation greatly enhances as the distance increases. Lastly, since the condition d>>h_t, h_r results in a slight angle of incidence for the reflection, the reflection coefficient can be approximated by unity. All of these assumptions must be broken, which necessitates the use of a more detailed equation than the one used here [38].
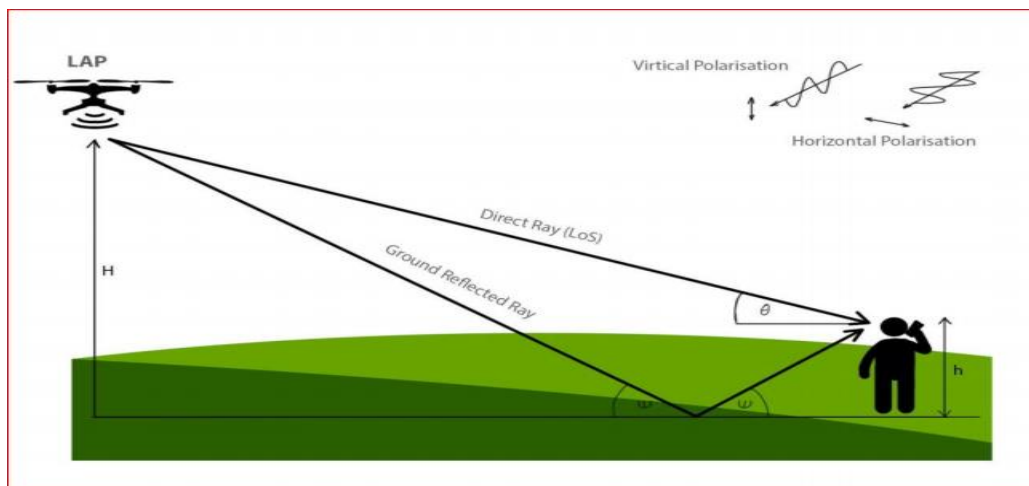
Figure 2.6: Two-ray model mean path loss in air to-ground channel. [63]

Chapter Three

Measurement and Simulation Setup for Indoor environment

3.1 Introduction

In the next few years, mobile radio communication services will increase significantly, according to the statistics and forecasts of some organizations. In particular, the demand for indoor services will be the key growth factor, which will account for more than half percent of the entire offering. While there are several indoor coverage technologies, such as wireless local area networks (WLAN) and femtocells, they all face issues in fulfilling the expanding demands. Several factors influence indoor propagation, which would be more adaptable than outdoor propagation. The architecture of the building has become increasingly diverse, posing significant challenges in categorizing and defining indoor scenarios. In addition to the conventional variables like frequency, walls and flooring often provide attenuations to indoor propagation [64].

In this chapter, simulation and measurements of the path loss indoor yard inside the Department of Communication Engineering building were compared. The theoretical analysis containing the simulation study using the Wireless InSite^{TM} software package (Remcom Company/USA) was the first part of this chapter. The second part of the study is experimental measurements to determine the path loss from a receiver operating at 3.5 GHz.

3.2 Simulation and Measurement Setup

Since measurements are often limited in some way (e.g. in frequency and number of places), we use the RT method to simulate the

channel environment. The simulation software used for this is Wireless Insite (WI) and its outputs include path loss, dispersion of delay, angular data, and Doppler shift.

3.2.1 Simulation Setup

3.2.1.1 Data about the building under investigation

The case study used in this thesis focuses on the corridor area in second floor of Communication Engineering Department/Electronics Engineering College building. The building was planned and simulated to use software Wireless InSite [65]. Initially, the environmental floor plan was set up in Wireless InSite, where an indoor floor plan is drawn directly with pre-defined materials as shown in Figure 3.1.
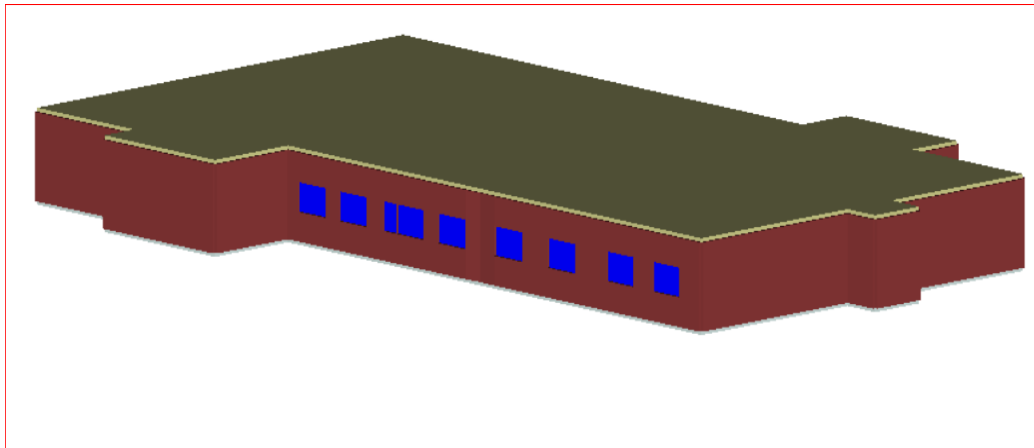
-a-
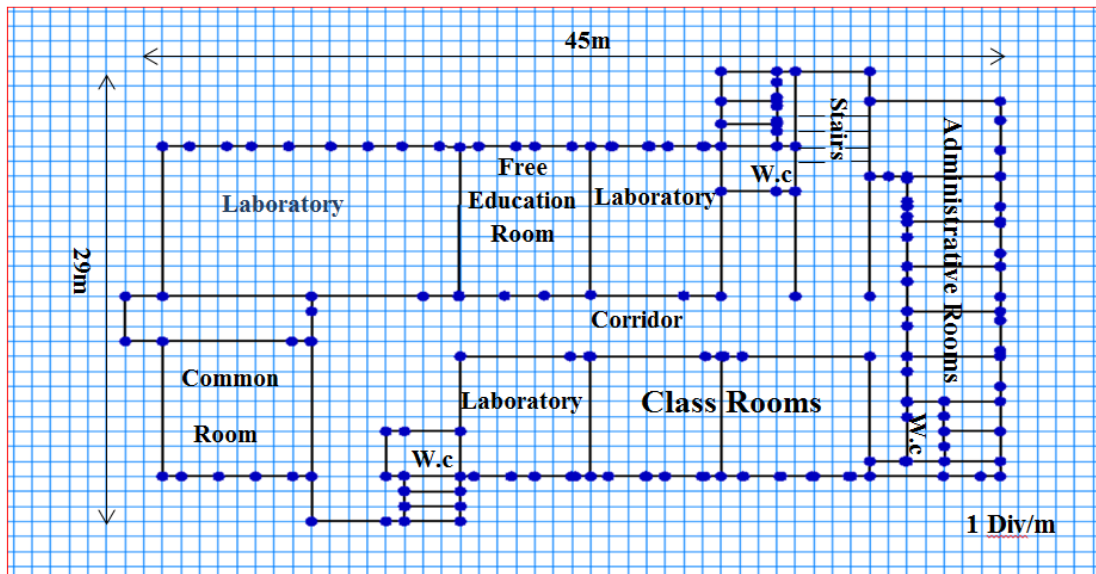
-b-

Figure 3.1: (a) Three-dimension view of the second floor, (b) Top view of
the second floor.

After configuring the floor plan, material parameters are added in. It
is possible to identify many material forms; we mainly use two types at
the present level: layered dielectric and perfect electrical conductor
(PEC). In indoor channel simulation, layered dielectric materials are used,
Such as the concept of walls, ceilings and floorboards for plasterboard as
shown in Table 3.1. Permittivity, conductivity, roughness, and thickness
of each layer of material must be given by the experiment data. The PEC
material is used to approximate good conductors, where transmission
coefficients, roughness and thickness are all set to zero (such as metal
exterior structures, elevator shafts and doors). For the corridor, three
materials are used for our indoor calibration: Plasterboard, mosaic tiles on
the ceiling, and concrete for floor.

Table 3.1: Specs of the construction of the communication engineering department/Ninevah University, which were taken into account in simulation and measurement. [26]

Height of Floor	3.5m
Thickness of walls	27cm
Materials of ceiling	1cm false ceiling panels+50cm air gap+ 15cm concrete layer +10cm mosaic tiles
Material of floor	Concrete+ mosaic tiles (30cm*30cm)
Material of walls	Brick covered by plaster ($\varepsilon_r = 4.44$, $\sigma=0.001$)
Material of doors	Plywood for most rooms, two parallel Sheet of iron separated by 3cm for laboratories
Material of windows	Glass of 4mm thickness, with iron grid of 30cm*30cm

3.2.1.2 Transmitter and Receiver Specifications

In our measurements, omnidirectional $\lambda/_4$ monopole antennas with gain (2dBi) were used at 3.5GHz frequency band. The transmitted power was ($\overline{+}$2dBm). Both of the antennas are oriented vertically polarized. The antenna patterns of both antennas are shown in the Figure 3.2 (In simulation, maximum gain orientation is adapted accordingly).
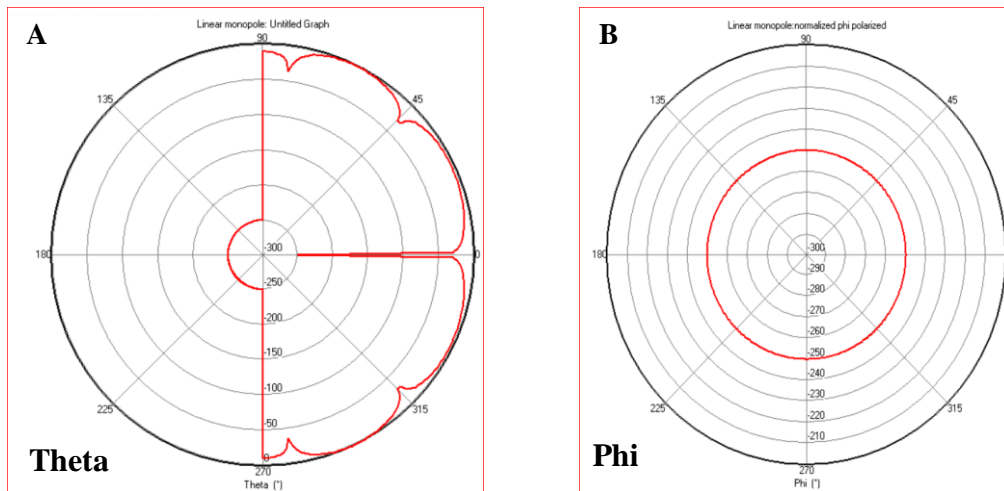
Figure 3.2: Radiation pattern for the antennas of Tx and Rx; (A) Vertical plane, (B) Horizontal plane.

3.2.1.3 Waveform Specifications and Study Area

With regard to waveforms used in simulation, sinusoid is used for 3.5GHz and 28GHz as shown in Figure 3.3, in compliance with measurements. In general, the limits of the study area are set as full (3D) SBR. For the majority of simulation situations, we use 6 reflections, 4 transmissions and 1 diffraction, respectively and dispersion diffuse is inactivated and number of propagating rays are 1-25, with acceptable simulation accuracy and simulation time. Simulation time is reduced: from 2 hours to 6 minutes, for example, if the number of diffractions decreases from 1 to 0.0.
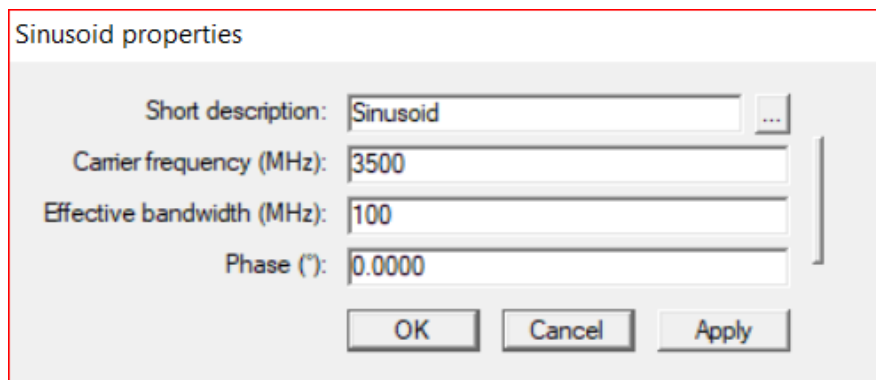
-a-
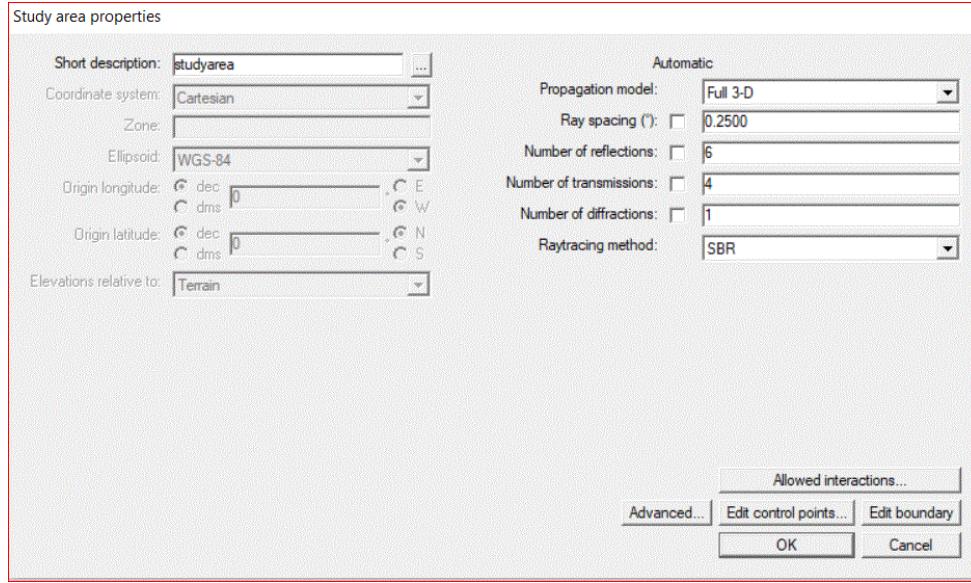
-b-

Figure 3.3: (a) Waveform of ray tracing model, (b) Study area of ray tracing model.

3.2.1.4 Outputs

Different output types are given by WI, but in this thesis one of them has been used which is described in equation (3.1).

$$Pr = \sum_{i=1}^{N_P} P_i = \sum_{i=1}^{N_P} \frac{\lambda^2 B}{8\pi\eta_0} |E\theta_i(\theta_i,\phi_i) + E\phi_i, \phi_i(\theta_i,\phi_i)|^2 \qquad (3.1)$$

Where N_P represents the number of paths, in this thesis it is taken as 469, in our stationary channel, which is sufficient. Parameter P_i is the average time of the ith path power in watts, which is constant for our stationary channel, λ is the wavelength of the signal; η_0 is the free impedance of space. The position of arrival in (elevation) and (azimuth) are θ_i and $\emptyset_i$ Ingredients, the $E_{\theta i}$ and $E_{\emptyset i}$ are the electrical field components of the elevation and azimuth of the i_{th} direction at the receiver, and β is an intersection of the transmitted waveform frequency spectrum and the waveform received, that lies within the [0, 1] interval.

Received power is then converted from watts to dBm and it is then possible to measure the path loss via,

$$PL\ (dB) = P_t\ (dBm) - P_r\ (dBm) + G_t\ (dBi) + G_r\ (dBi) - L_s\ (dB) \quad (3.2)$$

Where P_L in dB is path loss, P_t in dBm is the transmitted power, P_r in dBm is received power, antenna gains in dB are transmitted and received by G_t and G_r, and L_s is the loss of cables in dB [10].

3.2.2 Measurement Setup

In this work, one channel measurement method is used; focusing on 3.5 GHz. Figure 3.4 displays the 3.5 GHz channel measurement system that has been used.
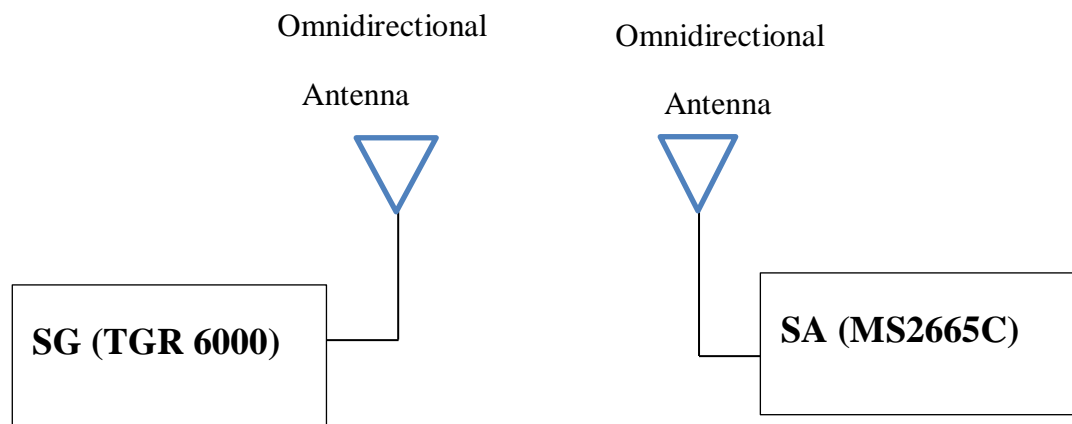
Figure 3.4: Channel measurement system.

A 2dBi gain monopole antenna is linked directly to the SG as Tx. With attenuator connected between TX and RX instead of antennas to measure the transmitted power producing power of 2 dBm. The SG is a fast-sweep 6GHz RF signal generator model TGR 6000 (10MHz to 6000MHz frequency range) as shown in Figure 3.5. In order to measure the maximum capacity of the receiver, the vector signal generator (VSG) was programed to transmit a narrow band signal with a 100 MHz bandwidth and maximum power of 2 dBm. The signal was delivered from the VSG to the signal spectrum analyzer (SSA) via cable.
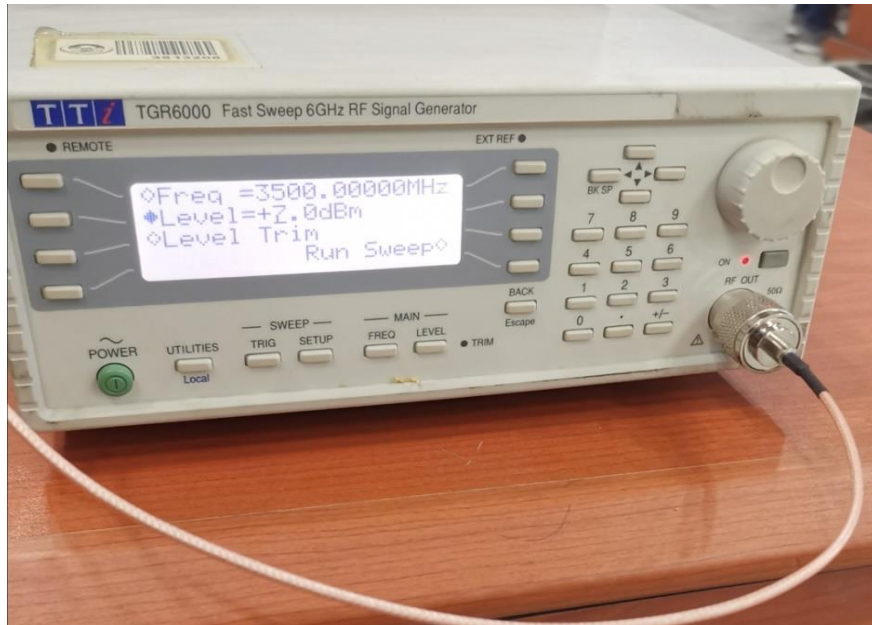
Figure 3.5: 6GHz RF signal generator.

Another similar monopole antenna has been connected directly to signal spectrum analyzer (SSA), with Anritsu model number MS2665C (9 KHz-21.2GHz frequency range) as shown in Figure 3.6; that was the Rx. For link to the antennas, coaxial transmission cables were used. The antennas were $\frac{\lambda}{4}$ omnidirectional antenna (operation band from 2.4 to 3.5 GHz) as shown in Figure 3.7; placed at a height of 1.34 meters relative to the ground. Vector signal generator (VSG) and signal spectrum analyzer (SSA) were both mounted on movable equipment carts. By putting the receiver 0.02m from the transmitter, a reference power level was determined. Co-polarization reference calculation was performed at this distance; co-polarized denotes when both transmitter and receiver antenna are vertically polarized for both LOS and NLOS cases.

Figure 3.6: Anritsu spectrum analyzer.
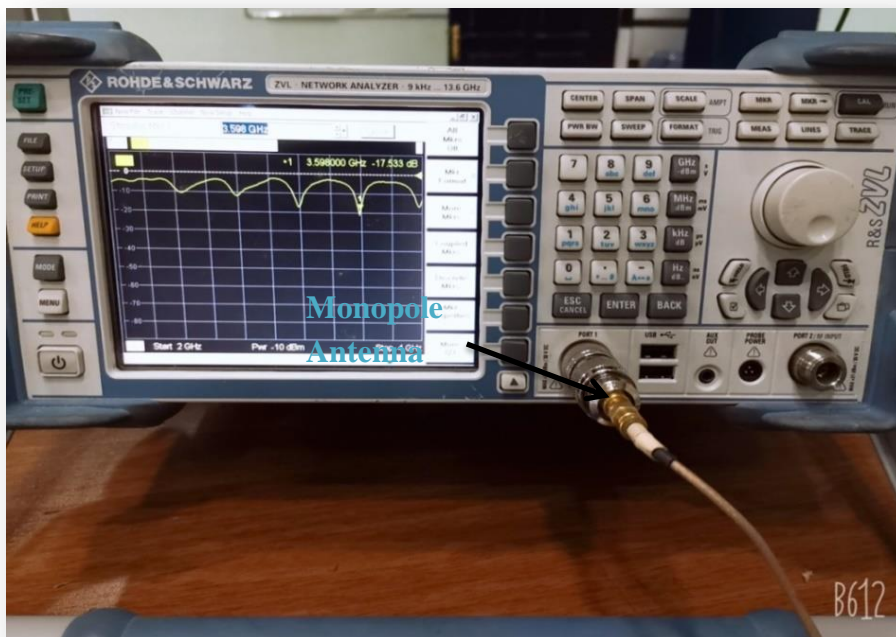
Figure 3.7: λ/4 Monopole antenna.

Both measurements and simulations campaigns were performed in the line of sight (LOS) channel condition when nothing blocked the path between the transmitter and the receiver, while the path between the

transmitter and the receiver is blocked in the Non-line of sight (NLOS) condition as shown in Figures 3.8 and 3.9.
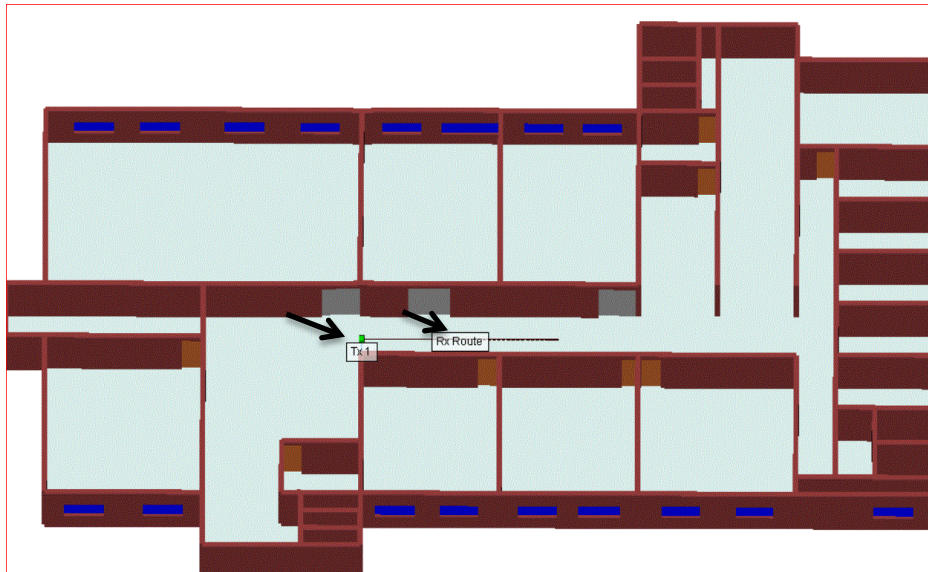
-a-
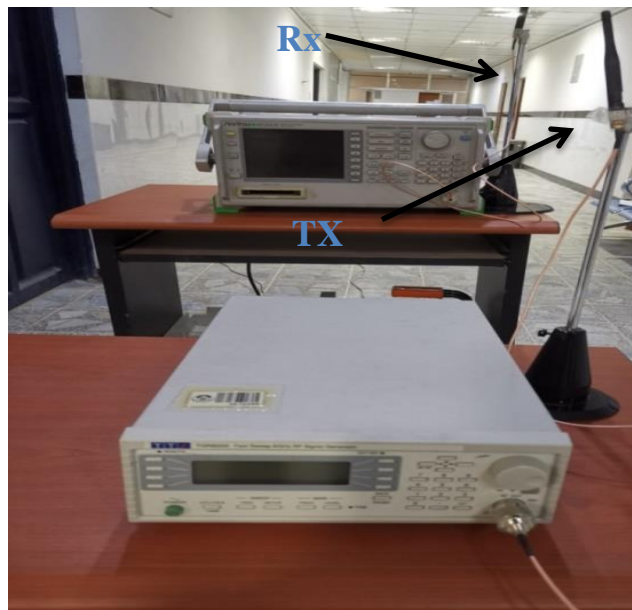
-b-

Figure 3.8: (a) Three-dimension simulation setup for LOS Case, (b) Indoor measurement setup for LOS case along the corridor.
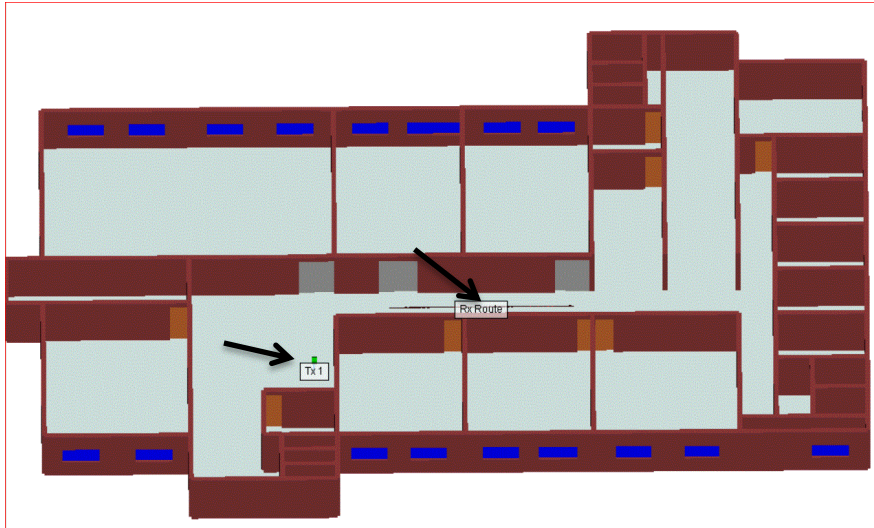
-a-

-b-

Figure 3.9: (a) Two-Dimension simulation setup for NLOS case (b) Indoor measurement setup for NLOS case along the corridor.

Chapter Four

Results and Discussion for Indoor Measurements

4.1   Introduction

The following results refer to both LOS and NLOS channel conditions. In Microsoft Excel [®], each dataset has been structured and processed in Matlab for evaluation and plotting. An example of path loss versus distance for simulation and long-corridor measurement of the 3.5 GHz method in both LOS and NLOS cases are shown in Figures 4.1 and 4.2. Overall, while more variance exists in practical measurements, the agreement is good. During practical measurements, the transmitter is steady and the receiver is shifted away in steps from 0.02 to 10 meters assuming single path.
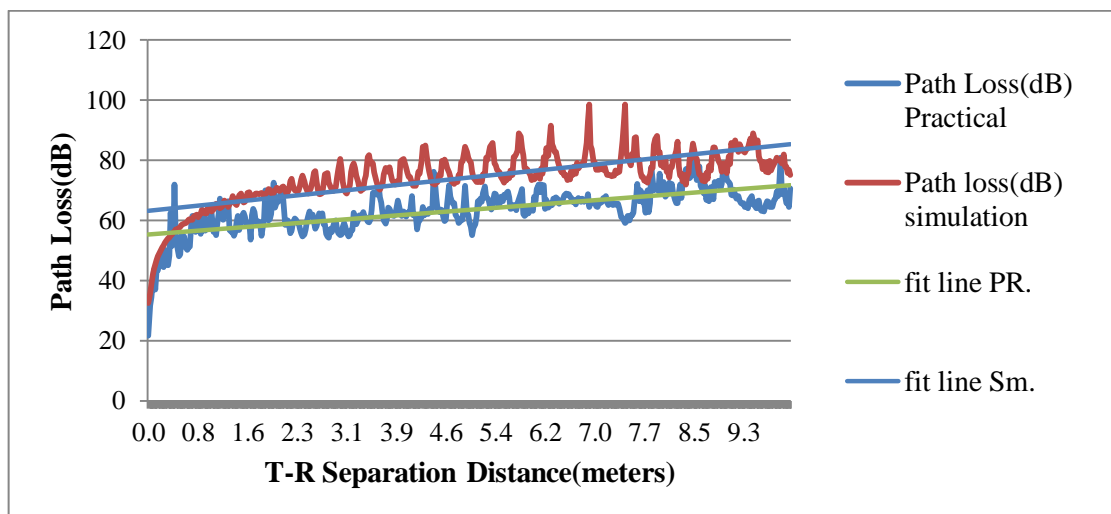
Figure 4.1: Measured and simulated path loss for the LOS case along the corridor with curve fitting.
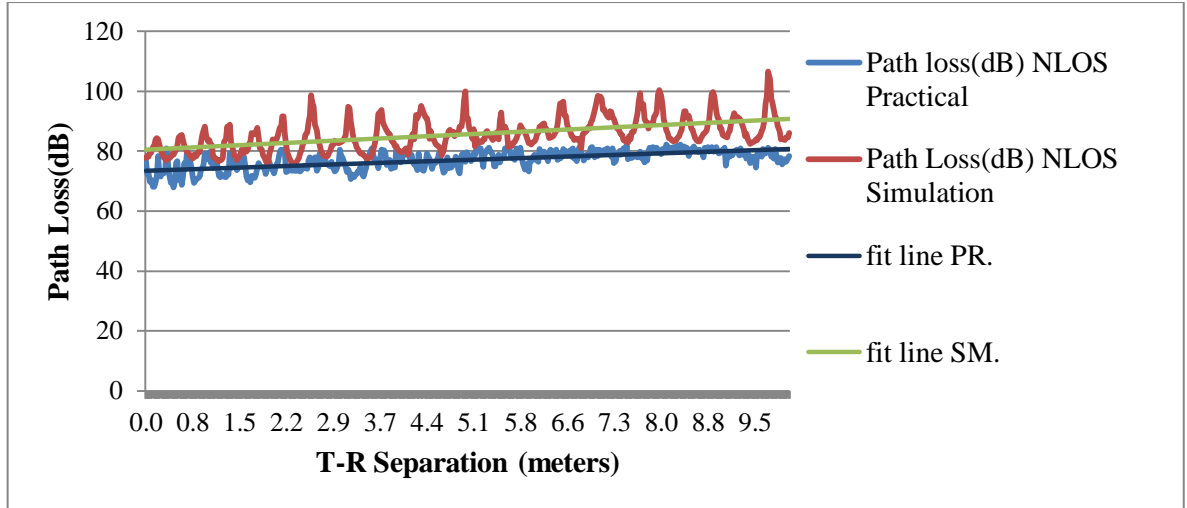
Figure 4.2: Measured and simulated path loss for the NLOS case along the corridor with curve fitting.

In measurements, the path loss calculation used is shown in equation (4.1) as mentioned in chapter 3:

$$L_{path} (dB) = P_T(dBm) - P_R (dBm) + G_T (dBi) + G_R (dBi) - L_S (dB) \qquad (4.1)$$

P_T and P_R are transmitted and received power, respectively, where G_T and G_R indicate maximum transmitting and receiving antenna gains, and L_S denotes other system losses, such as cable losses or losses of conversion, as alluded to in sub-section 3.2.1.4. To evaluate the consensus of simulation and measurement performance, the CI and FI path loss models are used. In WI, similar calculations are carried out.

4.2 Indoor Corridor Path Loss Modeling: Close-in Free Space Reference Distance Path Loss Model

The modeling technique used to characterize the 3.5 GHz LOS and NLOS data is known as the path loss model of Close-In free space reference distance (CI) [29]. The measurement, simulation, least squares (LS) fit to the results, CI model for the LOS setting in the building along the corridor as shown in Figures 4.3 and 4.4.

According to the equation was mentioned in chapter two.

$$PL_{CI}\ (f_c,\ d)\ [dB]\ =FSPL\ (f_{c,}\ d_0)\ [dB]\ +\ 10n log_{10}\ d/\ d_0\ +\ X_\sigma \qquad (4.2)$$

For, $d > d_0,\ where\ d_0 = 1\ m.$
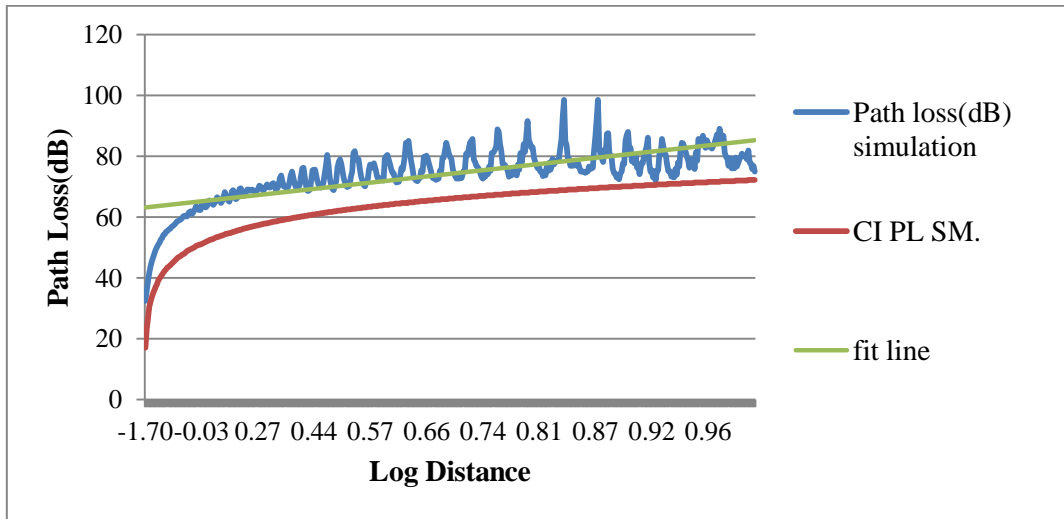
Figure 4.3: CI path loss model, simulation path loss vs. Log distance along the corridor for LOS case.
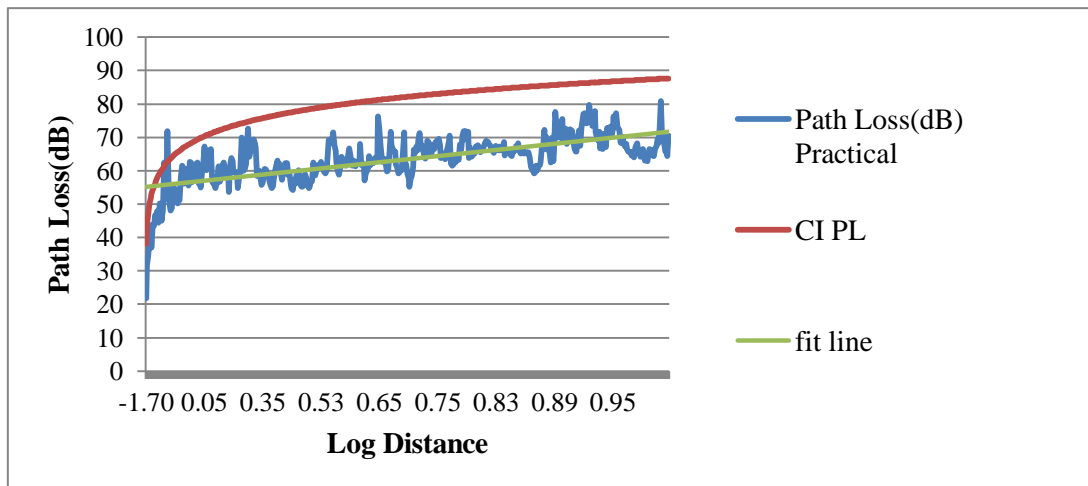
Figure 4.4: CI path loss model, measurement path loss vs. Log distance along the corridor for LOS case.

The same findings are shown in Figure 4.5 after integrating data from Figures 4.3 and 4.4.
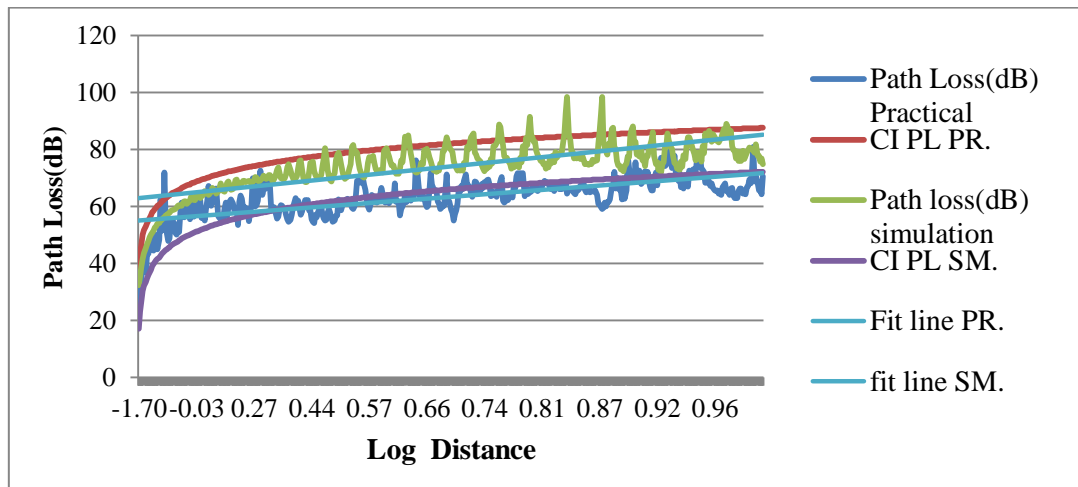
Figure 4.5: Combined measurement and simulation path loss vs.
Logarithm of distance, along the corridor for LOS case.

For LOS case, comparison of results for local measurement data with simulation data results, it can be observed that the n and σ_{CI} differences between simulation and measurement are not greater than 0.2 and 1.75 dB, respectively. It's clear that both values for LOS case in measurement and simulation are very close to each other. The small difference between them, is possibly attributable to several factors affected each of the runs performed during the measurement; such as imprecise pattern of the antenna or imperfect placement of the Tx/Rx in WI where the Tx/Rx might not be located in the exact position as the measurement. The variations can also be contributed because of the material parameter inaccuracies and neglect of diffraction, but these should be secondary and also in the simulation, software chooses the best propagation path unlike practical measurement. Parameters for the CI model are shown in Table 4.1.

Table 4.1: Parameters for the CI model in LOS case.

LOS Case	PLE(n)	Standard Deviation σ_{CI} dB	No.of Points
Simulation	2.04	1.05	25
Measurement	1.83	3.86	43

Non-line of sight (NLOS) measurements was made in the same corridor after LOS measurements had been completed. The transmitter was located at the corner of the corridor for these NLOS measurements; the receiving antenna was positioned 90° apart from the transmitting antenna to ensure there was no LOS path. The measurement, simulation, least squares (LS) fit to the results, CI model for the NLOS setting in the building along the corridor, are shown in Figures 4.6 and 4.7.
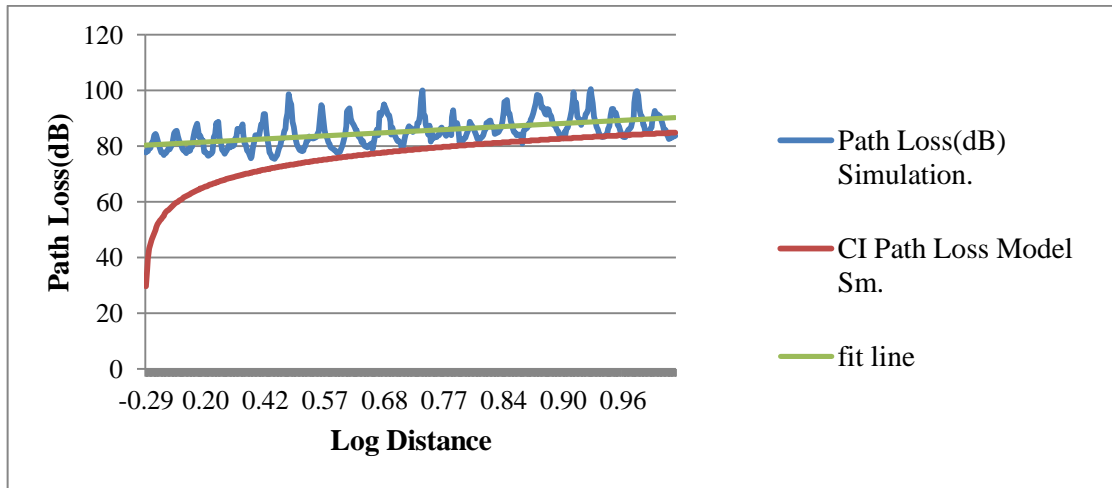
Figure 4.6: CI path loss model, simulation path loss vs. Log distance along the corridor for NLOS case.
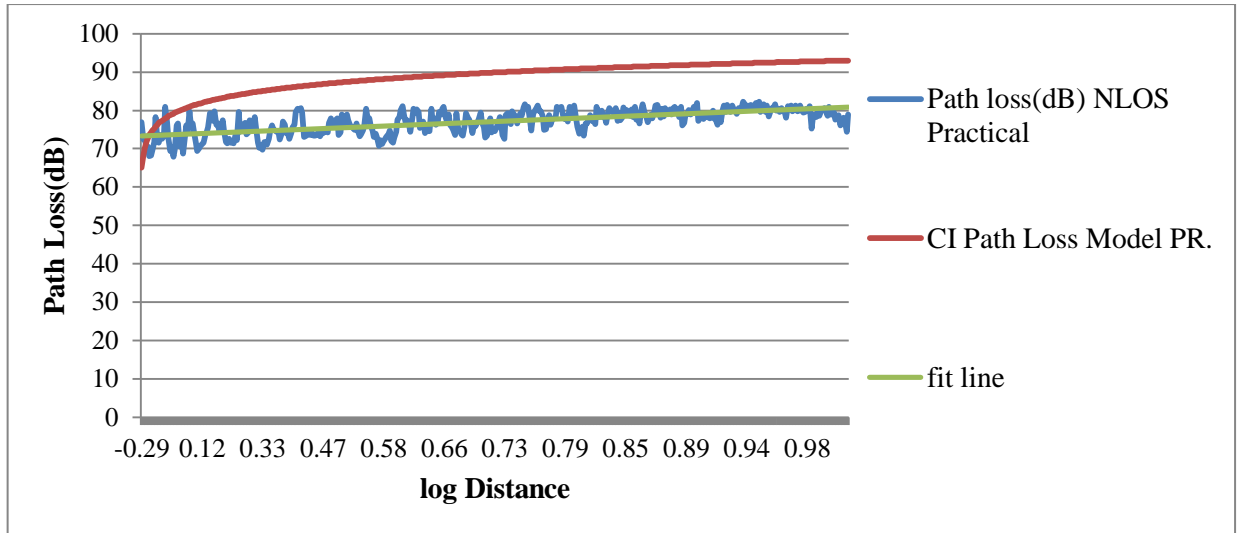
Figure 4.7: CI path loss model, measurement path loss vs. Log distance
along the corridor for NLOS case.

The same findings are shown in Figure 4.8 after combining data from
Figures 4.6 and 4.7.
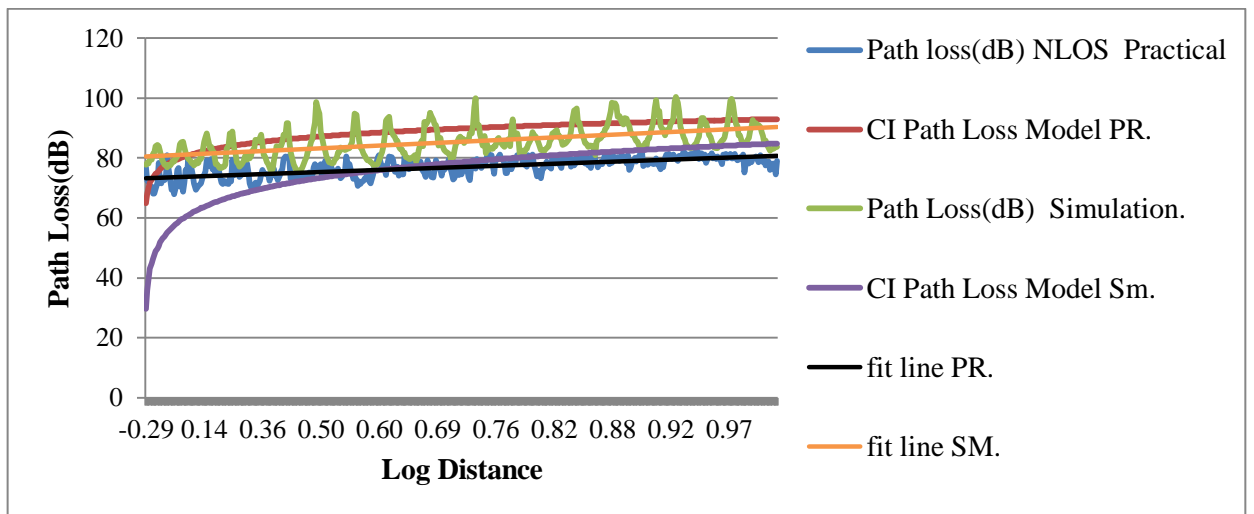
Figure 4.8: Combined measurement and simulation path loss vs.
Logarithm of distance, along the corridor for NLOS case.

According to CI model for NLOS case, the variation in n is 0.02dB
between simulation and measurement; the path loss exponent (n) is larger
than the value of measurement, while difference in σ_{CI} is 2.10 dB
between the simulation and measurement as shown in below Table 4.2.

Table 4.2: Parameters for CI model in NLOS case.

NLOS Case	Path loss exponent (n)	Standard Deviation σ_{CI} dB	No.of Points
Simulation	2.06	5.23	44
Measurement	2.04	3.13	59

The path loss exponent (n) in NLOS case is larger than LOS by 0.23dB for simulation and 0.28 dB for measurement.

4.3 Indoor Corridor Path Loss Modeling: Floating-Intercept Path Loss Model

The results of the FI model are described as the following equation which is mentioned in chapter two.

$$PL_{FI}(d) = \alpha_0 + 10\beta log\ 10(d) + X_{\sigma FI} \qquad (4.3)$$

The practical measurements, simulation, least squares (LS) fit to the results, FI model for the LOS and NLOS cases in the building along the corridor are shown in Figures 4.9 and 4.10.
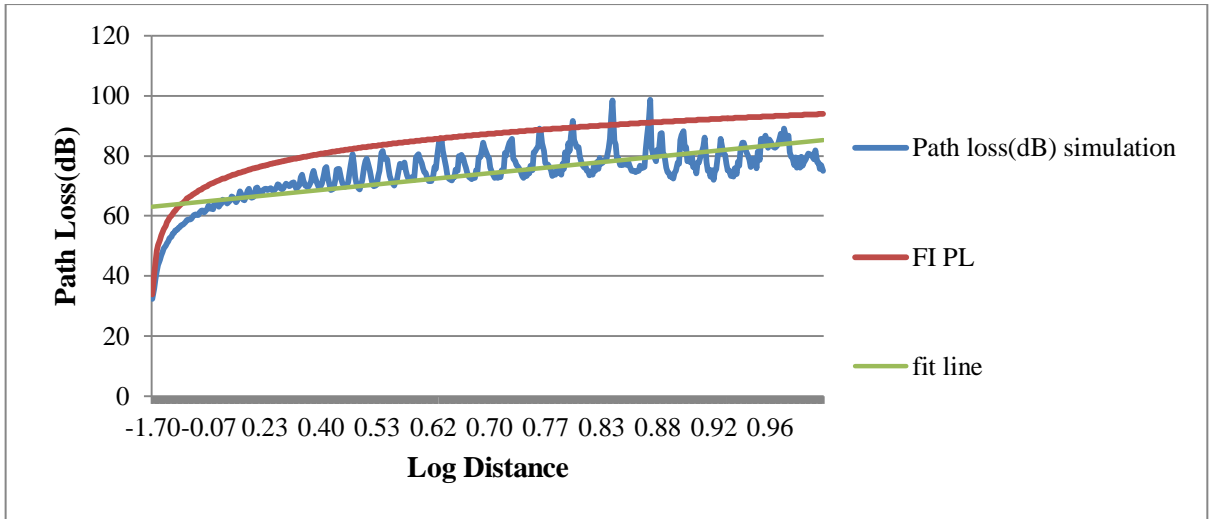
Figure 4.9: FI path loss model, simulation path loss vs. Log distance
along the corridor for LOS case.
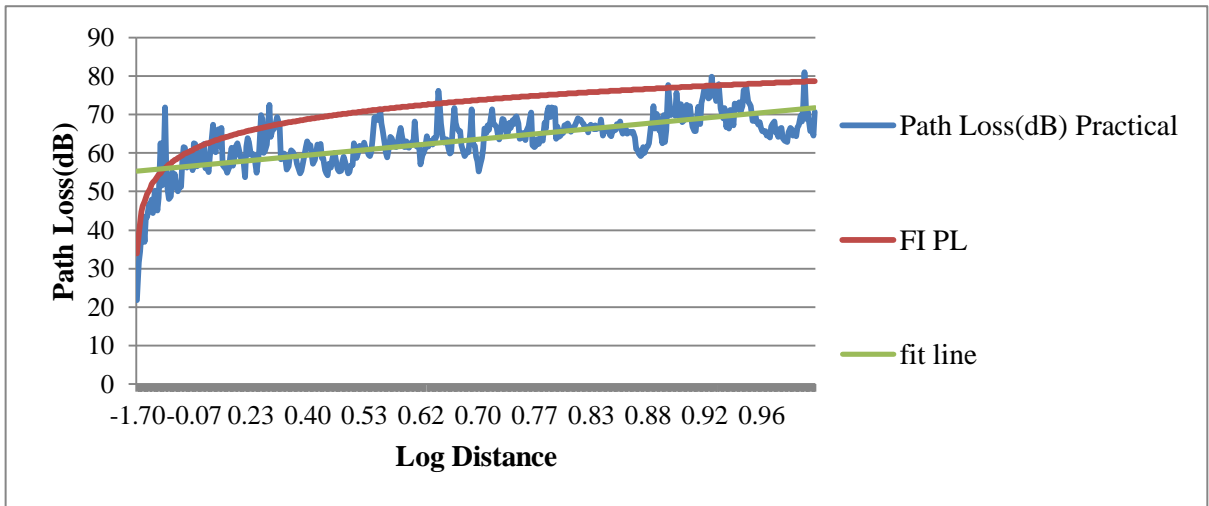
Figure 4.10: FI path loss model, measurement path loss vs. Log distance
along the corridor for LOS case.

The same findings are shown in Figure 4.11 after integrating data
from Figures 4.9 and 4.10.
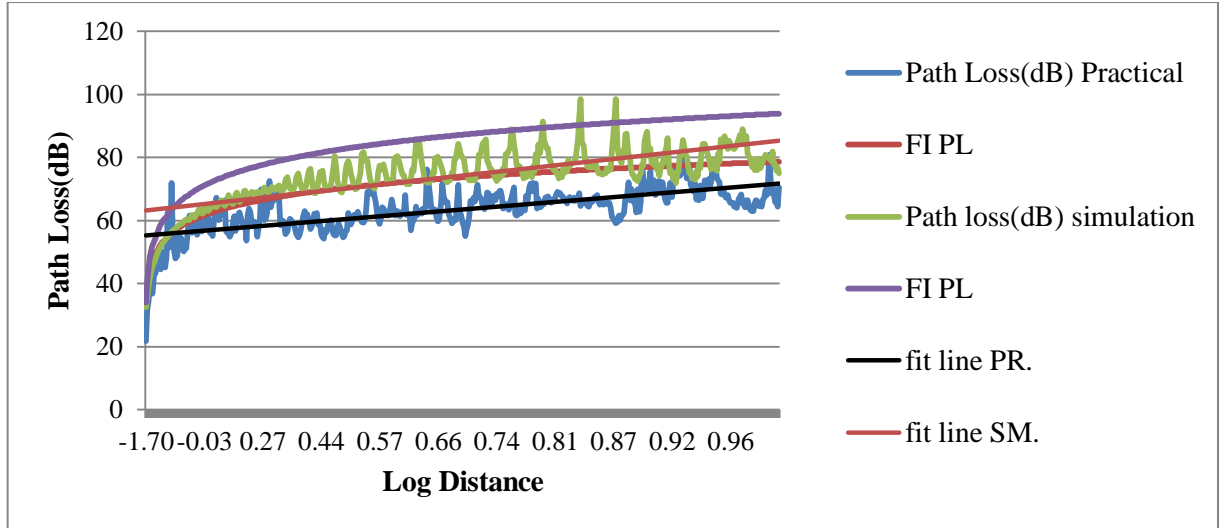
Figure 4.11: Combined measurement and simulation path loss vs. logarithm of distance, along the corridor for LOS case.

The FI parameters, α, β and σ_{FI}, for simulation and measurement are shown in Table 4.3. α,β and σ_{FI} variations in the FI model between simulation and measurements values are larger than 7dB, 0.5, 1.7dB, respectively. The values of α in both simulation and measurement are larger than that of free space path loss FSPL which is theoretically 43.39dB. Slope value (β) of the minimum-square mean fit line for the case LOS for simulation method is larger than that of free space ($\beta = 2$) while close to the free space in the measurement method.

Table 4.3: Parameters for FI model in LOS case.

LOS Case	α(dB)	β	σ(dB)
Simulation	63.07	2.22	6.91
Measurement	55.20	1.65	8.62

Path losses for the NLOS channel, FI model are shown in Figures 4.12 and 4.13.
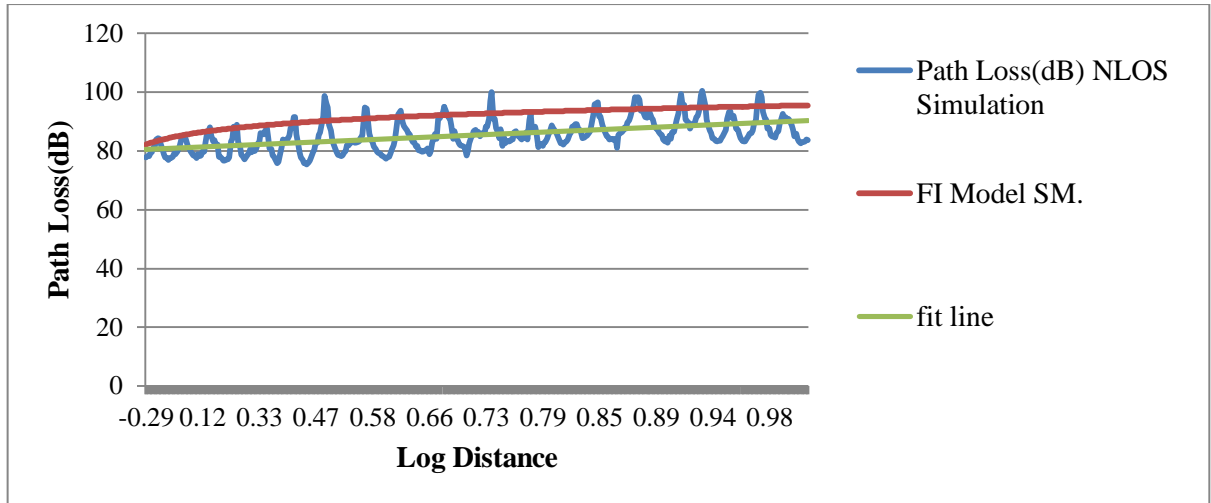
Figure 4.12: FI path loss model, simulation path loss vs. Log distance along the corridor for NLOS case.
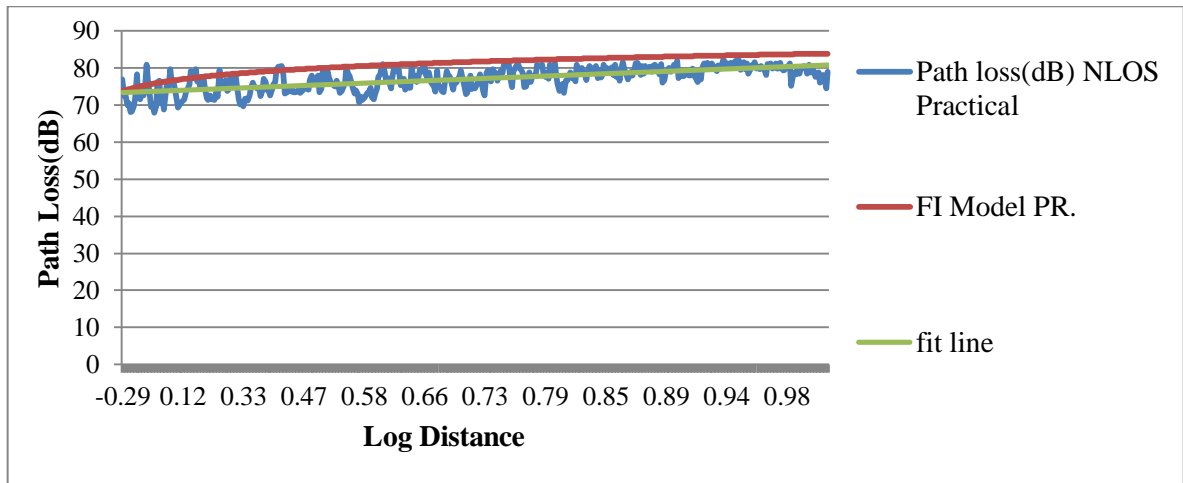
Figure 4.13: FI path loss model, measurement path loss vs. Log distance along the corridor for NLOS case.

Combining figures 4.12 and 4.13 to get Figure 4.14 shown to compare between two methods.
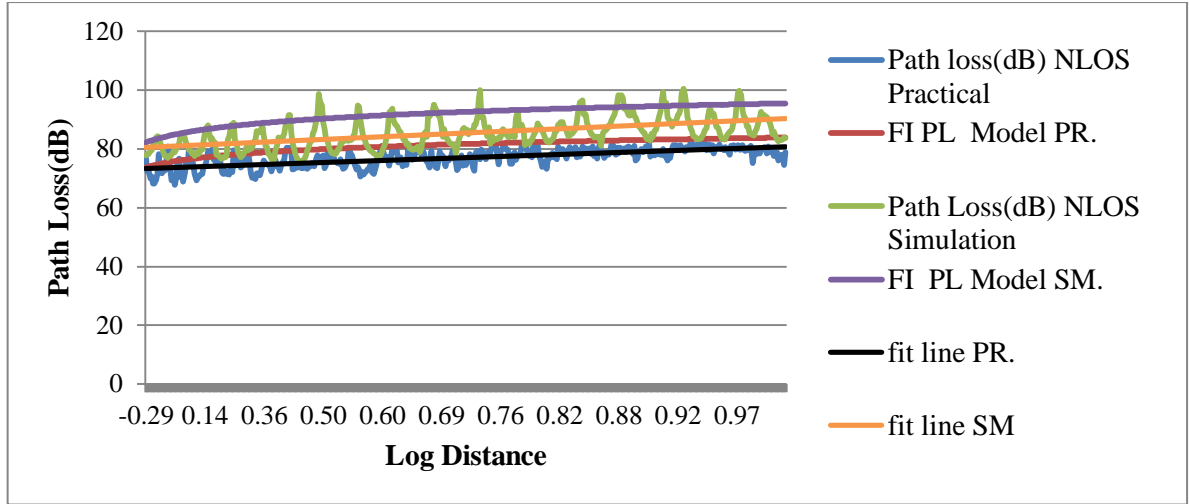
Figure 4.14: Combined measurement and simulation path loss vs. logarithm of distance, along the corridor for NLOS case.

Differences in α, β and σ_{FI} between simulation and measurement results for the NLOS case are less than 7dB, 0.2 and 2dB respectively. As shown in the Table 4.4, it can be seen that α value is very large compared to the free space path loss FSPL (FSPL=43.39dB) theoretical with respect to the LOS case owing to the unavailability of a clear path in the NLOS condition study. β slope value in both methods are less than that of free space (β=2) because it merely serves as a basic slope for determining the best fit for a data line plot and has no physical basis or frequency dependency in any way. This does not imply that NLOS signals have higher distance attenuation than that of free-space transmissions.

Table 4.4: Parameters for FI model in NLOS case.

NLOS Case	α dB	β	σ dB
Simulation	79.91	1.03	5.25
Measurement	73.51	0.78	3.13

The NLOS path loss case is approximately 13.5 dB greater than the LOS case for both simulation and measurement results. A better antenna

pattern agreement is one possible explanation, due to its simple structure, the monopole antenna patterns used in WI simulation agree much better with real monopole antenna patterns used in measurement. The results show that the difference of the path loss exponent (n) parameter changes dramatically when a brick wall corner blocks the direct connection between transmitter and receiver, forcing NLOS conditions.

The value of the path loss exponent for simulation (by Wireless InSite software) and measurement results was found to be within the range of recorded values when compared to recent works by [66], [67] and [68] as indicated in Table (4.6). In reference [66] for modern multi-story buildings in various areas, measurements were taken at various frequencies of (433-2400) MHz. Both the Tx and Rx antennas were adjusted to a height of 50cm. N. Rakesh et al. [67] computed the path loss exponent from measurements data (for urban Macro cell scenario) at three frequencies of 3.35, 4.9, and 5.4GHz at base station antenna, it is mounted on the rooftop of a building fixed with a telescopic tower, and mobile station antenna, which is connected to a tower setting up on the top of a van used during the calculation. Furthermore, in reference [68] within the range (3.1-4.2), the path loss exponent was found for seven various frequencies and different rooms.

Table 4.5: Comparison of path loss exponent with most recent works in indoor environments.

Environment	Frequency range GHz	Path Loss Exponent (n)	Channel Conditions
Narrow Straight Corridor(measurement)[66]	2.4	2.10	LOS
Wide Straight Corridor (simulation)[66]	2.4	1.43	LOS
Urban Micro Cell(measurement)[67]	3.35	3.32	NLOS
Multi-room [68] residential(measurement)	3.6-3.7	4.4	OLOS
Urban Micro Cell(measurement) [67]	4.9	2.07	LOS
Urban Micro Cell(measurement)[67]	5.4	2.06	LOS
Urban Micro Cell(measurement)[67]	5.4	3.60	NLOS

Chapter Five

Path Loss effects on Millimeter and Centimeter Waves in Outdoor Environment

5.1 Introduction

Estimating path loss of channel parameter is important for modeling fifth generation communications systems over distance and/or frequency in outdoor wireless cellular systems [69]. A significant amount of attenuation due to vegetation, atmospheric gases, a high blockage loss due to human body and many other obstacles commonly found in outdoor environments are the main outdoor propagation characteristics [70].

In this chapter path loss and channel modeling were evaluated at the outdoor environment with respect to the sub-band and millimeter band using ray tracing technology, the simulation software used for this was Wireless Insite® (WI).

5.2 Simulation of the Study Area

The Wireless InSite software was used to create a simulation model for the campus of the Electronics Engineering College in Mosul as shown in Figures 5.1 and 5.2, which was then executed upon seeing its actual dimensions depend on Google Earth Map (GEM) software. Table 5.1 lists all of the materials that were used to establish the model.

Table 5.1: Materials of the study area

Type of Material	Thickness
Brick	0.125
Wet Earth	0.000
Foliage	0.000500

The transmitter is situated at a height of 2.0 meters above ground level. In addition, this study employs a specific type of receiver known as a route. As shown in Figures 5.1 and 5.2, the number of points deployed on campus is 39, all of which are considered LOS because there are no barriers between them and the transmitter. Also the height of the receiver is 1.70 m from the ground.
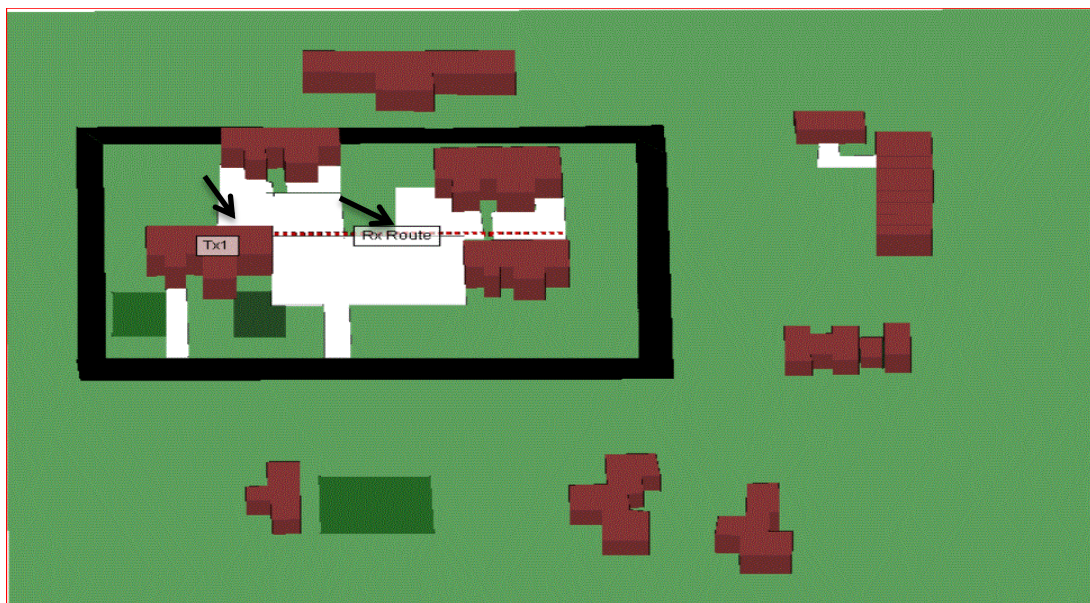
Figure 5.1: Three-dimension structure for the study area designed using the Wireless InSite.

Figure 5.2: Simulation scenario of electronics engineering college area Using GEM.

5.3   Antennas for the Study Area

Both the transmitter and receiver use directional and omnidirectional antennas taking into consideration the effect of the types of polarization, as shown in Figures 5.3 and 5.4.

A

B
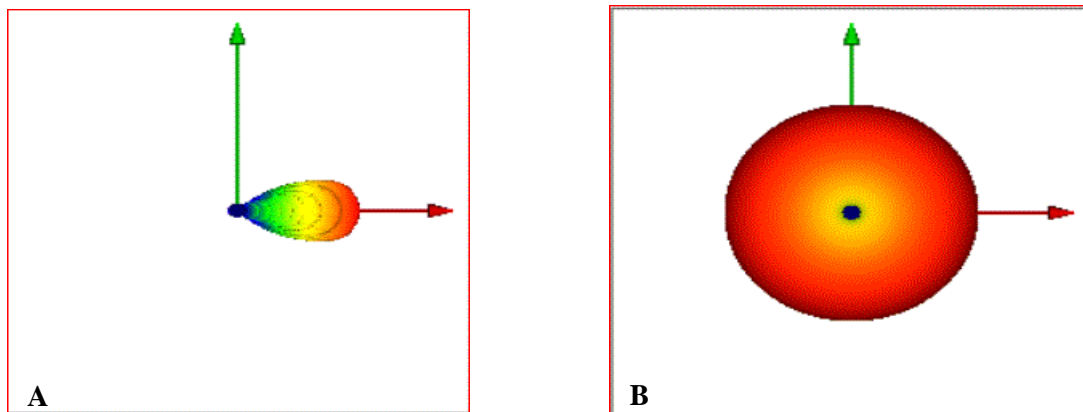
Figure 5.3: Radiation pattern of antennas for (A) directional and (B) omnidirectional at vertical polarization.
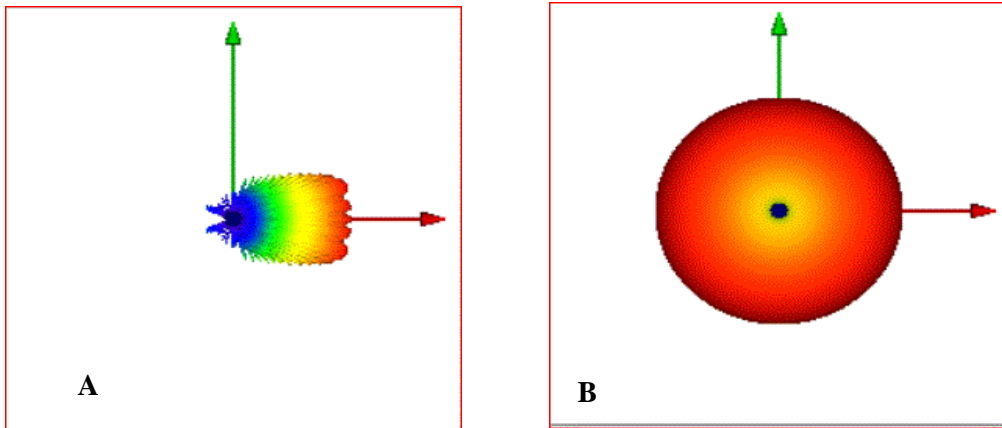
Figure 5.4: Radiation pattern of antennas for (A) directional and (B) omnidirectional at horizontal polarization.

Properties of both the transmitting and receiving antennas are presented in the Table 5.2. For our case study, we chose a bandwidth of 100MHz for 3.5GHz and 1GHz for 28GHz.

Table 5.2: Characteristics of the directional and omnidirectional antennas at 3.5GHz and 28GHz.

Parameter	3.5GHz	28GHz
Horn Transmit power(dBm)	26.00	30.00
Antenna Gain(dBi)	9.80	24.5
Omni-directional Transmit Power(dBi)	10.00	10.00
Transmit Antenna Gain(dBi)	2.5	8.50
Receiver Antenna Gain(dBi)	1.47	4.76
Horn-omnidirectional Transmit power(dBm)	26	20.00
Transmit Antenna Gain(dBi)	9.6	19.18
Receiver Antenna Gain(dBi)	2.0	Auto
Transmitter Height(m)	2.00	2.00
Receiver Height(m)	1.70	1.70
Bandwidth(MHz)	100	1000

5.4   Results

The Path Loss models are important for predicting the attenuation of signals propagating over long distances. The close-in (CI) free space reference distance model and the floating-intercept (FI) (alpha-beta) model are two of the most commonly used empirical path loss models are used for comparison between 3.5 and 28GHz frequency bands for directional and omnidirectional antennas.

5.4.1   Close-In Free Space Reference Distance (CI) Path Loss Model

Simulation and Close-In path loss model results for 3.5GHz for directional antenna with the effect of co-polarization and cross-polarization are depicted in Figure 5.5.
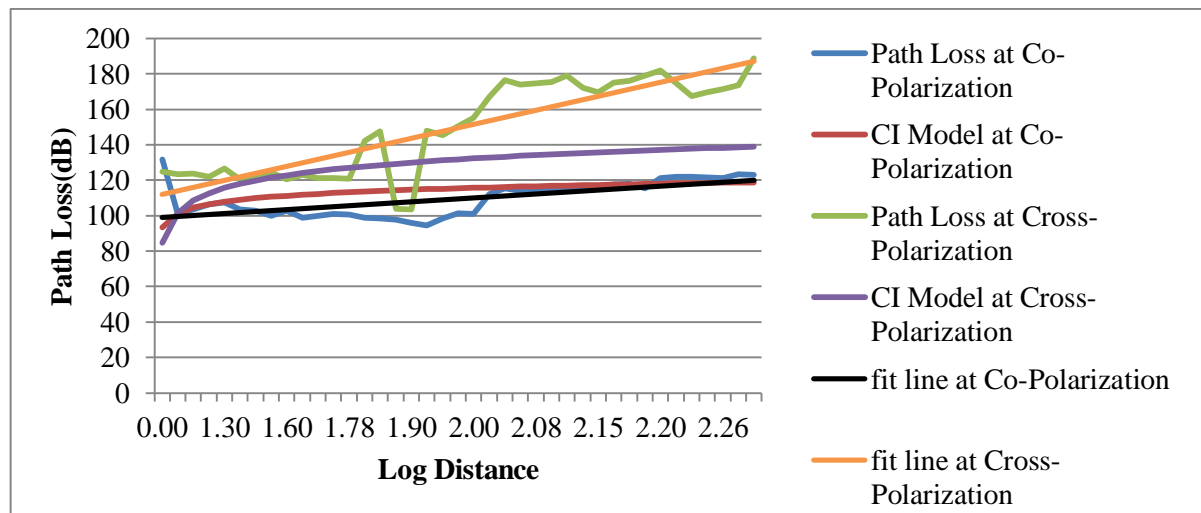
Figure 5.5: CI path loss model, simulation path loss vs. Log distance for horn antenna at co-polarization and cross-polarization for outdoor environment at 3.5GHz.

For LOS scenario at the 3.5GHz frequency band, comparison of simulation results of path loss models for different types of antennas with effect of both polarizations. For co-polarization and cross-polarization it can be observed that the path loss exponent (n) compared to the free space path loss exponent (n=2) and standard deviation σ_{CI} values are

different. For horn antennas PLEs values are smaller than free space value of 2 for co-polarization. On the contrary, the PLE value is larger than 2 for cross-polarization because of mismatch polarization so that in this case there is additional loss in the signal. Large-scale signal variations are defined by standard deviation (σ_{CI}). The σ_{CI} values have difference of 0.94 dB/decade between two cases of polarizations. Whereas when using omnidirectional antennas the path loss exponent (n) value is larger than free space path loss exponent (n=2) for both polarizations because of low gain of antenna compared to the horn antenna. The σ_{CI} values for cross-polarization are larger than co-polarization by 1.03dB/decade. Also σ_{CI} for omnidirectional antenna are larger than that of horn antenna for both polarizations because of the height gain of horn antennas as depicted in Figure 5.6.
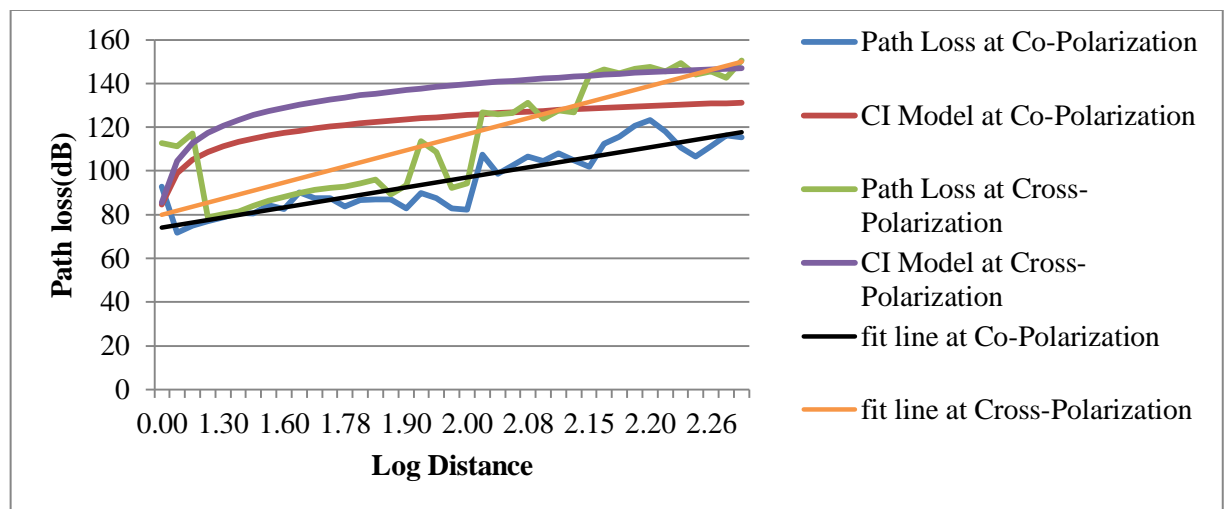
Figure 5.6: CI path loss model, simulation path loss vs. Log distance for omnidirectional antenna at co-polarization and cross-polarization for outdoor environment at 3.5GHz.

Meanwhile when using horn antenna for transmitter and omnidirectional for the receiver the path loss exponent (n) values for both types of polarizations is also larger than that free space path loss exponent (n=2)value but less than omnidirectional antennas. Also the σ_{CI} values for

cross-polarization and co-polarization are different by 0.85dB/decade as shown in Figure 5.7.
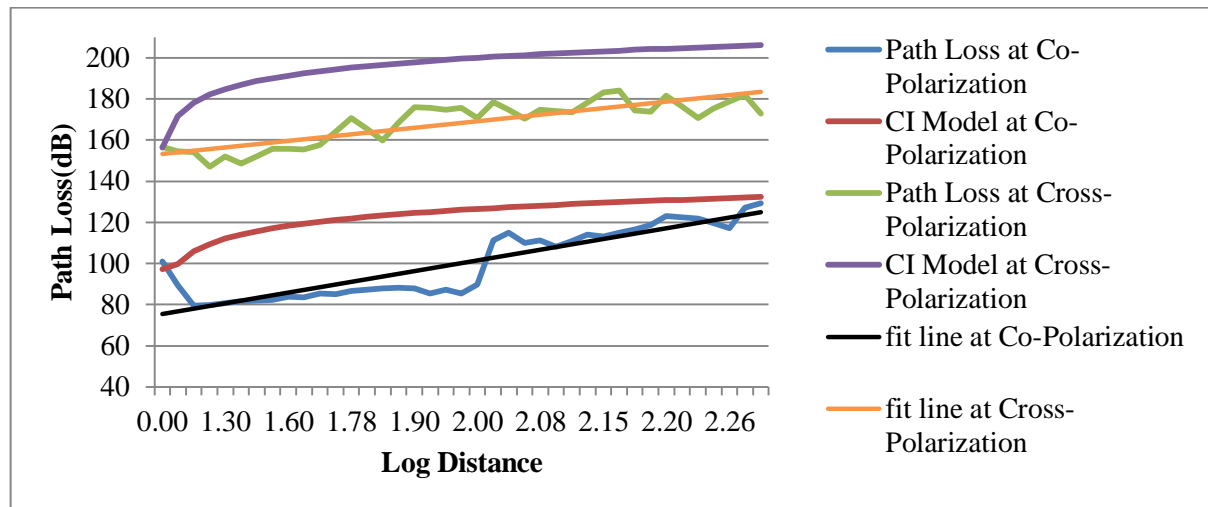
Figure 5.7: CI path loss model, simulation path loss vs. Log distance for horn- omnidirectional antenna at co-polarization and cross-polarization for outdoor environment at 3.5GHz.

The parameters of the Close-In path loss models for directional, omnidirectional and horn-omnidirectional antennas at 3.5GH frequency band are shown in Table 5.3.

Table 5.3: Parameters of the Close-In path loss models for directional and omnidirectional antennas at 3.5GHz frequency band.

Antenna Types	Polarization	PLE (n)	σ (dB)
Horn	**V-V**	1.87	0.98
	V-H	2.37	0.92
Omnidirectional	**V-V**	2.05	1.04
	V-H	2.70	2.07
Horn-Omni	**V-V**	2.07	1.35
	V-H	2.18	2.20

For the other frequency in mm wave band (28GHz frequency band) which is also one of the candidate frequencies for fifth generation cellular system. The Close-In (CI) path loss model and simulation results are shown in the figures (5.8-5.10). These results of different types of antennas are display by different colors with the fitting line for co-polarization and cross-polarization to distinguish them. For horn antennas as seen in the Figure 5.8.the path loss exponent (n) values are close to the free space path loss exponent (n=2) for co-polarization. On the contrary the PLE value for cross-polarization is higher than co-polarization. The σ_{CI} value is different by 0.14dB/decade for cross-polarization and co-polarization as shown in the Table 5.4.
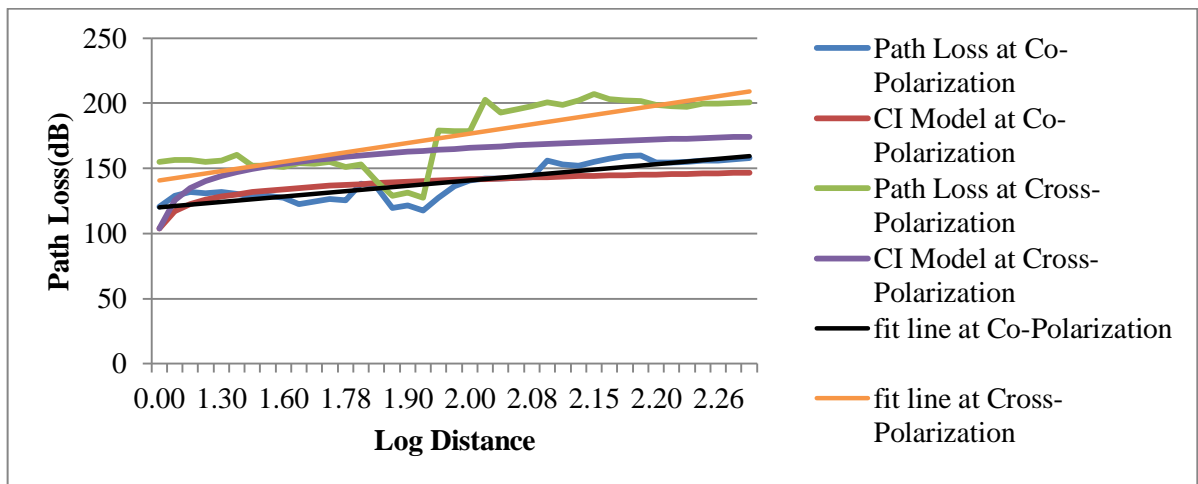
Figure 5.8: CI path loss model, simulation path loss vs. Log distance for horn antenna with co-polarization and cross-polarization for outdoor environment at 28GHz.

For omnidirectional antennas the CI path loss model results and simulation results are shown in Figure 5.9. The path loss exponent (n) values for both polarizations are higher than of free space path loss exponent (n=2) value. In the omnidirectional antennas the multipath increases when using high frequency so that the PLEs values increase.

65

The σ_{CI} values for cross-polarization are larger than co-polarization by 0.48dB/decade.
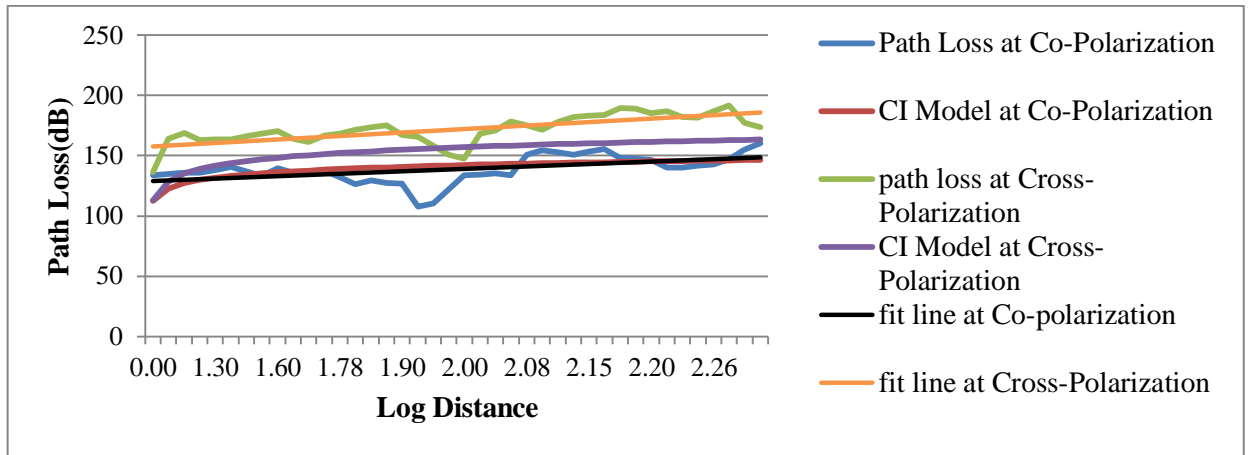
Figure 5.9: CI path loss model, simulation path loss vs. Log distance for omnidirectional antenna at co-polarization and cross-polarization for outdoor environment at 28GHz.

Figure 5.10 shows the tacking effect of horn-omnidirectional antennas. For both types of polarizations, the path loss exponent (n) values were higher than the free space path loss exponent (n=2) value. Also, the outdoor LOS PLE (n=3.49) value for cross-polarization was higher than the outdoor LOS PLE value for the 3.5GHz band because of the higher frequency. The σ_{CI} values have different trends for both types of polarizations. The standard deviation σ_{CI} values of cross-polarization differ by 1.02dB/decade than co-polarization. The parameters for Close-In path loss model for horn, omnidirectional and horn-omnidirectional for 28GHz frequency band are shown in the Table 5.4.
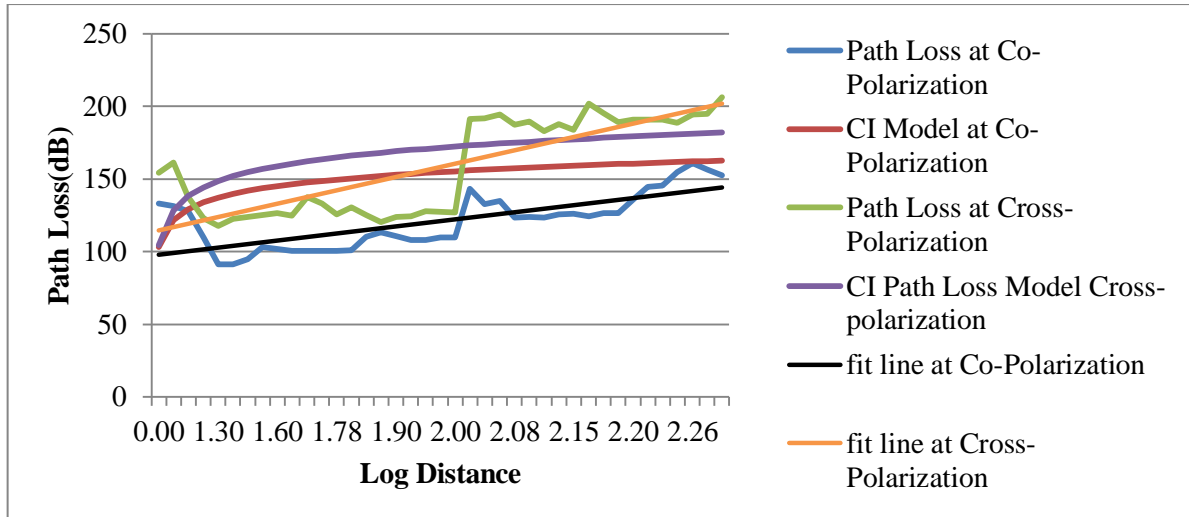
Figure 5.10: CI path loss model, simulation path loss vs. Log distance for horn-omnidirectional antenna at co-polarization and cross-polarization for outdoor environment at 28GHz.

Table 5.4: Parameters for Close-In path loss model for directional and omnidirectional for 28GHz frequency band.

Antenna Types	Polarization	PLE (n)	σ (dB)
Horn	V-V	2.00	2.10
	V-H	3.1	2.24
Omnidirectional	V-V	2.5	1.14
	V-H	3.26	1.62
Horn-Omni	V-V	2.64	1.81
	V-H	3.49	2.83

Comparing Figures (5.5-5.10) for 3.5 and 28GHz, the PLEs were found to be nearly identical for co-polarization cases for horn antennas and close to the free space path loss exponent. However, whereas the omnidirectional and horn-omnidirectional antennas, PLEs values in the 3.5 and 28 GHz frequency band were higher than free space path loss

exponent(n=2) at both polarization cases, because of the low gain of omnidirectional antennas. The figures show that path loss at 3.5 GHz and path loss at 28 GHz have strong consistency. It can be concluded that the 28 GHz PLE values are always greater than the 3.5 GHz PLE values at the same place, and this result holds true for all polarizations in LOS scenarios. The PLEs values for cross-polarization at 28 GHz is obviously around 7.3 dB higher than at 3.5 GHz for horn antenna and 5.6dB for omnidirectional and 13.1dB for horn-omnidirectional antennas.

5.4.2 Floating-Intercept Path Loss Model (FI)

Figures 5.11, 5.12 and 5.13 demonstrate the path loss model findings for directional and omnidirectional antennas with distances ranging from 1-190 meters, taking into account the influence of both polarizations in the 3.5GHz frequency band. For directional antenna, the parameters of the FI path loss model indicate that the PLE (β slope) is nearly identical to the CI model with 13.2dB less for co-polarization and 4.0dB for cross-polarization. For omnidirectional antennas the β slope value compared to the CI model was 9.0 dB less for co-polarization and 8.6dB for cross-polarization. Finally the PLE (β slope) value for the horn-omnidirectional antenna was 7.7dB for co-polarization and 3.9dB for cross-polarization, because of the slight difference between the references value at 100 m and the maximum FI path loss value at 190 m. This implies that the path loss slope was small, while the slope along the path loss in the CI model (the reference value is 1 m) was high in comparison to the 190 m path loss value. The floating intercept (α) value also compared to the theoretical free space path loss of (43.39dB) for directional antenna have difference 45.15and 63.61 dB/decade for co-polarization and cross-polarization respectively. Whereas for omnidirectional antenna the floating intercept (α) values have difference 29.57 and 34.76 dB/decade

for co-polarization and cross-polarization. Finally for horn-omnidirectional antenna the α values have difference 30.60 and 63.72dB/decade for co-polarization and cross-polarization respectively.
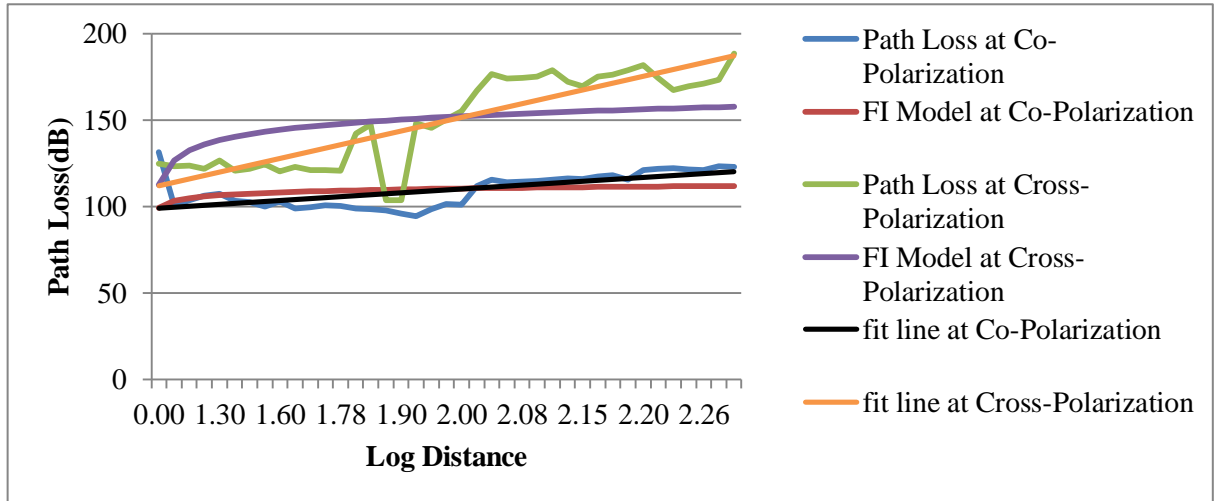
Figure 5.11: FI path loss model, simulation path loss vs. Log distance for horn antenna at co-polarization and cross-polarization for outdoor environment at3.5GHz.
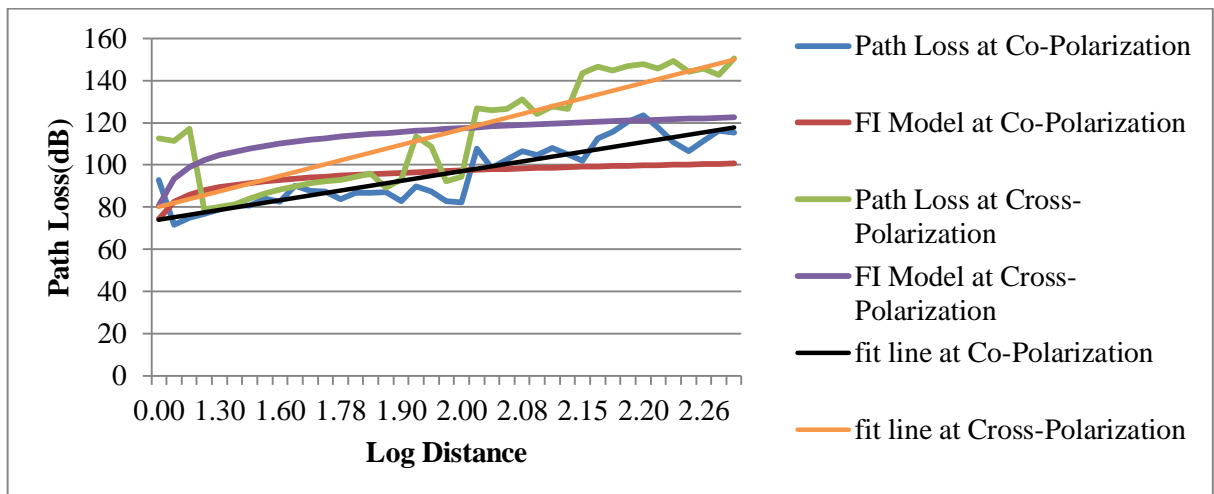
Figure 5.12: FI path loss model, simulation path loss vs. Log distance for omnidirectional antenna at co-polarization and cross-polarization for outdoor environment at 3.5GHz.

69
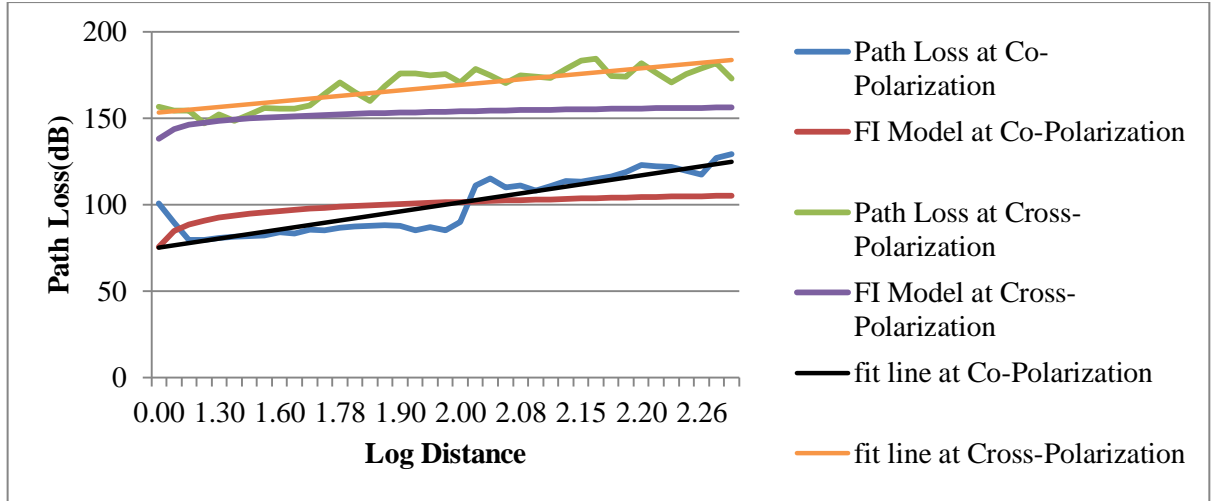
Figure 5.13: FI path loss model, simulation path loss vs. Log distance for horn-omnidirectional antenna at co-polarization and cross-polarization for outdoor environment at 3.5GHz.

The parameters of the FI path loss model are shown in the Table 5.5.

Table 5.5: FI path loss model parameters at 3.5GHz.

Antenna Types	Polarization	α(dB)	β	σ (dB)
Horn	**V-V**	88.54	0.55	0.99
	V-H	107.00	1.97	2.59
Omnidirectional	**V-V**	72.96	1.15	1.46
	V-H	78.15	1.84	2.46
Horn-Omni	**V-V**	73.99	1.30	1.66
	V-H	107.11	1.79	1.06

For 28GHz, the parameters of the FI path loss models are display in Table 5.6. The FI path loss model parameters for directional antenna also compared to the PLE (β slope) value is similar to the CI path loss model with 9.6 dB less for co-polarization and 13.1 dB less for cross-

polarization as shown in Figure 5.14. The (β slope) value for omnidirectional antenna was 11.8 dB less for co-polarization and 10.5dB less for cross-polarization as shown in Figure 5.15. Whereas for horn-omnidirectional antenna the results as shown in Figure 5.16. The β slope value was less than PLE in the CI model by 15.2dB for co-polarization whereas it was less than PLE value by 11.9dB for cross-polarization. The floating intercept values at 28GHz also compared to the theoretically free space path loss of (61.39dB) vary widely in all cases for antennas. As shown in case of directional antennas for both polarization cases the floating intercept (α) values have difference of 43.81 and 56.21 dB/decade for co-polarization and cross-polarization respectively. For omnidirectional antennas the α values have 27.29 and 29.63 dB/decade for co-polarization and cross-polarization respectively. Finally for horn-omnidirectional antennas the α values have 36.47 and 50.73 dB/decade for co-polarization and cross-polarization respectively. The standard deviation (σ_{FI}) values have different trends for different types of antennas. The σ_{FI} values increases at cross-polarization compared to the co-polarization is not higher than 2 dB at both antennas.
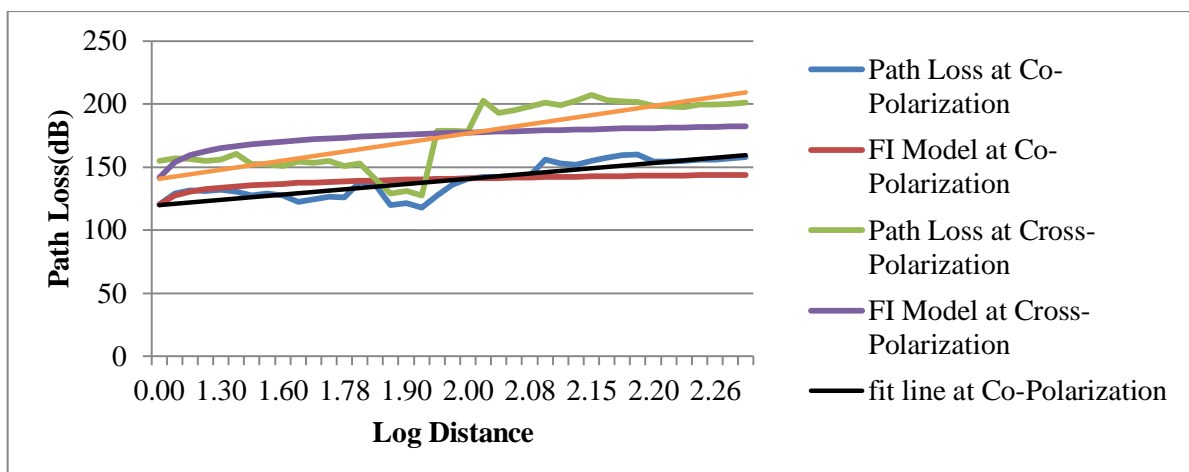
Figure 5.14: FI path loss model, simulation path loss vs. Log distance for horn antenna at co-polarization and cross-polarization for outdoor environment at 28GHz.
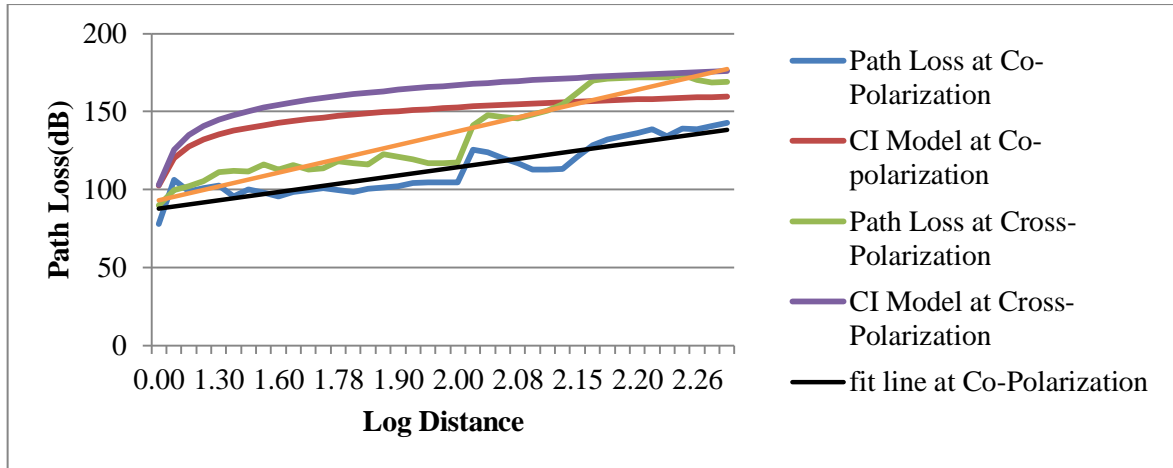
Figure 5.15: FI path loss model, simulation path loss vs. Log distance for omnidirectional antenna at co-polarization and cross-polarization for outdoor environment at 28GHz.
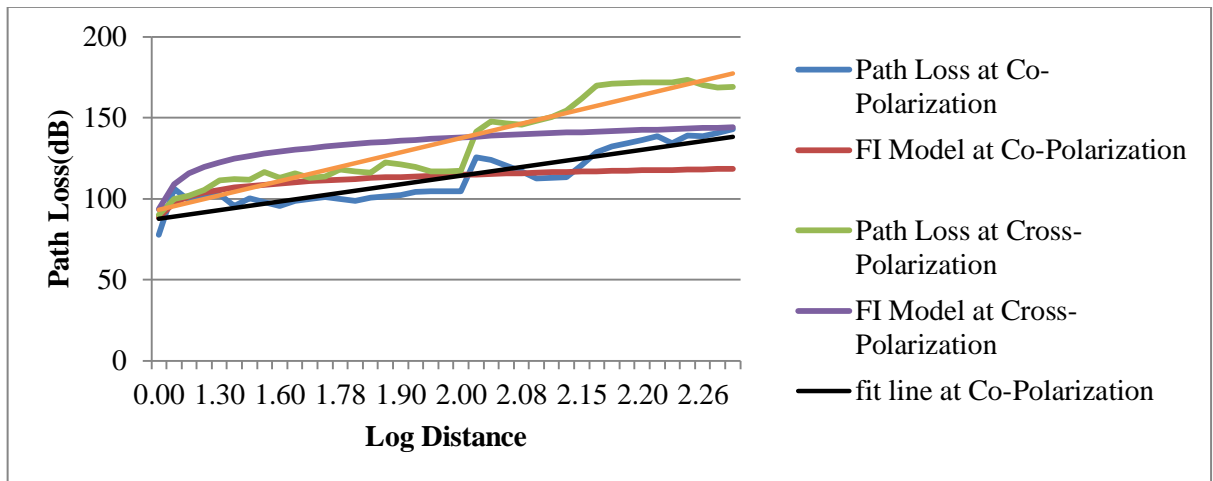
Figure 5.16: FI path loss model, simulation path loss vs. Log distance for horn-omnidirectional antenna at co-polarization and cross-polarization for outdoor environment at 28GHz.

Table 5.6: FI path loss model parameters at 28GHz.

Antenna Types	Polarization	α(dB)	β	σ (dB)
Horn	V-V	105.20	1.04	1.38
	V-H	117.60	1.79	2.05
Omnidirectional	V-V	88.68	1.32	1.65
	V-H	91.02	2.21	2.64
Horn-Omni	V-V	97.86	1.12	1.90
	V-H	112.12	2.30	3.26

As shown in Figures (5.11-5.16), the FI model demonstrated close reflection frequency dependence at 3.5 GHz and 28 GHz, respectively. This phenomenon is known as the wavelength effect, since when the wavelength is reduced, the rate of reflection increases proportionally. Finally, the FI model can be used to model a horn antenna for co-polarizations at 3.5GHz and 28GHz respectively, and it is highly recommended for the 28 GHz frequency band. The horn-omnidirectional antenna for co-polarization β **slope** line value at 3.5 GHz was higher than the slope line at 28 GHz. It is obvious the β slope line is not frequency dependency. Also it can be concluded that the path loss exponent (n) values depend on environment more than frequency dependence and distance dependence. The comparison between two Path loss models for different types of antennas at 3.5 and 28 GHz are shown in the Table 5.7.

Table 5.7: Single-frequency FI and CI path loss models in an outdoor scenario at 3.5GHz and 28GHz parameters.

Antenna types	Polarization	Frequency GHz	Model	PLE (n)	β	α (dB)	σ (dB)
Horn-Antenna	V-V	3.5	Cl	1.87	-	-	0.98
			Fl	-	0.42	88.54	0.99
		28	Cl	2.00	-	-	2.10
			Fl	-	1.04	105.2	1.38
	V-H	3.5	Cl	2.37	-	-	1.92
			Fl	-	1.97	107.0	2.59
		28	Cl	3.1	-	-	2.24
			Fl	-	1.79	117.60	2.05
Omnidirectional-Antenna	V-V	3.5	Cl	2.05	-	-	1.04
			Fl	-	1.15	72.96	1.46
		28	Cl	2.4	-	-	1.14
			Fl	-	1.32	88.68	1.65
	V-H	3.5	Cl	2.7	-	-	2.07
			Fl	-	1.83	78.15	2.46
		28	Cl	3.26	-	-	1.62
			Fl	-	2.21	91.02	2.64
Horn-Omni	V-V	3.5	Cl	2.07	-	-	1.35
			Fl	-	1.30	73.99	1.66
		28	Cl	2.64	-	-	1.88
			Fl	-	1.12	97.86	1.90
	V-H	3.5	Cl	2.18	-	-	2.20
			Fl	-	1.79	107.11	1.06
		28	Cl	3.49	-	-	2.83
			Fl	-	2.30	112.12	3.26

5.4.3 Alpha-Beta-Gama (ABG) Path Loss Model

The results of the simulation path loss compared to the ABG model for directional and omnidirectional antennas at 3.5, 28 and 38GHz in outdoor environment are shown in the following figures 5.17, 5.18 and 5.19. They show the path loss model for various frequencies and include factors that are affected by distance and frequency. The ABG multi-frequency model parameters are listed in Table 5.8. For the omnidirectional antenna the distance-coefficient term α is larger by 1.9

and 4.7dB/decade than for the directional and horn-omnidirectional antennas. This difference because of high multipath for omnidirectional antenna. The frequency-coefficient slope (γ) is 3.99, 3.39 and 1.7 for omnidirectional, horn-omnidirectional and horn antennas for LOS case study. The standard deviation σ value at horn-omnidirectional antenna is larger by 0.43 and 13.93dB/decade than omnidirectional and horn-omnidirectional antennas.
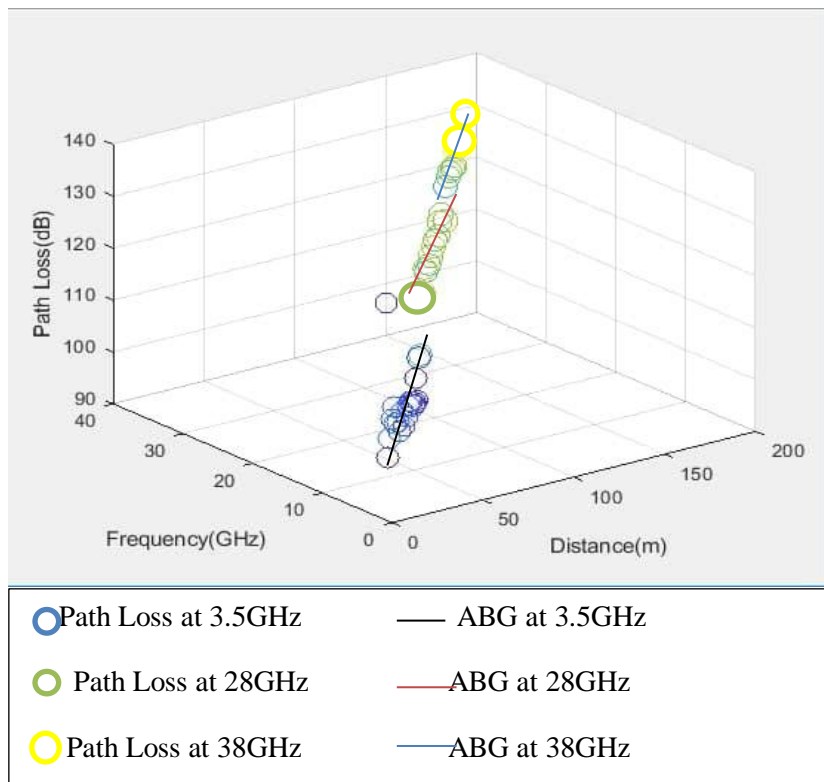
Figure 5.17: ABG path loss model for horn antenna at 3.5,28 and 38GHz.
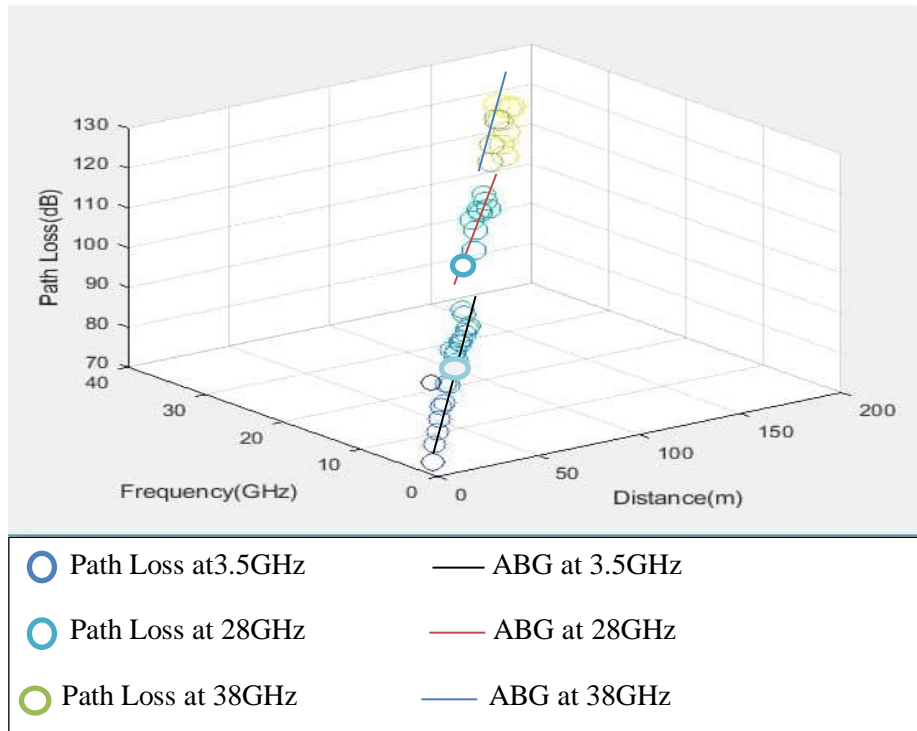
Figure 5.18: ABG path loss model for omnidirectional antenna for 3.5,28 and 38GHz.
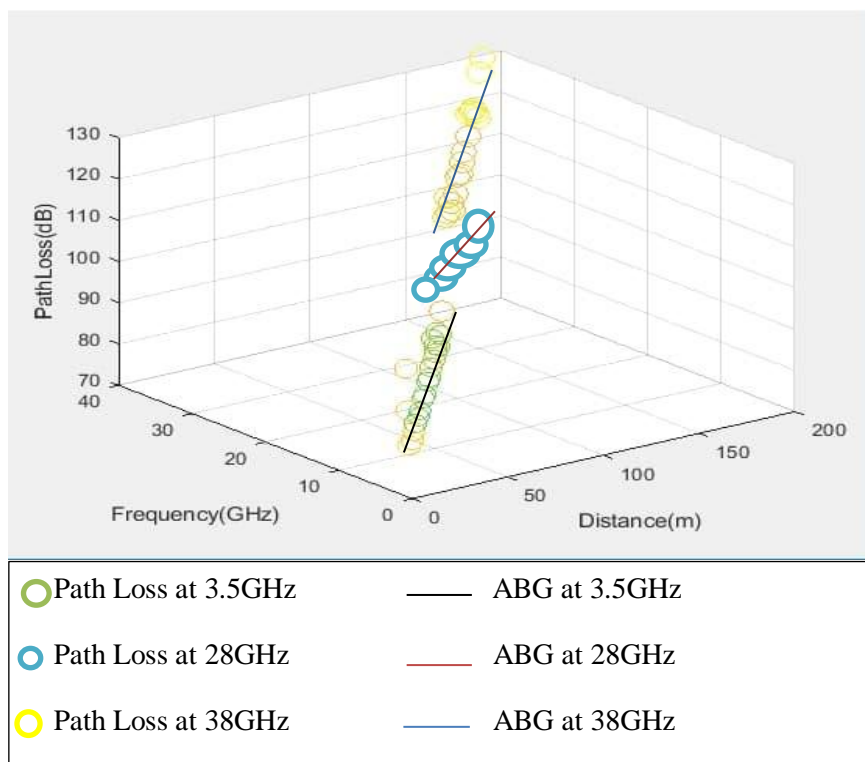
Figure 5.19: ABG path loss model for horn-Omni antenna at 3.5,28 and 38GHz.

Table 5.8: Parameters of ABG path loss model for 3.5,28 and 38GHz frequency bands.

Antenna Type	α	β	γ	σ(dB)
Horn	1.54	31.93	1.7	3.64
Omnidirectional	1.73	36.85	3.99	4.99
Horn-Omni	1.25	29.11	3.39	5.033

Table 5.9 shows comparison of different outdoor parameters in this work with similar recent works. In [70] the investigation was carried in an outdoor urban environment in a tropical country like Malaysia, where rain and fog were present, to examine and precisely quantify the co-polarization and cross-polarization attenuation factor from the perspectives of various antenna polarizations and scenarios. The measurement results show that the PLE (n) value for the CI model is higher than free space PLE value (n=2) for LOS and NLOS scenarios. On the contrary, in the ABG model the distance-dependency α value is 1.12 for the LOS and 2.38 for the NLOS at different frequencies. The results of [71] show that the PLE values at 3.5 and 28GHz are larger than free space path loss exponent value (n=2) for both LOS and NLOS conditions in urban macro-cellular (UMa) scenario. In [72] the path loss exponent (n) values for diverse parking lot scenarios were nearly comparable at 28 GHz and 38 GHz, according to the results. Also the standard deviation values for both single Park lot (SPL) and Dual Park lot (DPL) were virtually comparable, indicating that the shadowing effect was almost identical in both cases.

Table 5.9: Parameters of the path loss models for recent works for outdoor environment.

Scenarios	Frequency	Model	PLE (n_{CI},α_{ABG})	β_{Fl},β_{ABG}	α_{FI}	γ_{ABG}	σ_{Cl} dB	σ_{Fl} dB	σ_{ABG} dB
Urban environment	26	Cl	1.53	-	-	-	1.71		-
	28		2.71	-	-	-	4.18		-
	36		3.05	-	-	-	3.37		-
	38		3.12	-	-	-	3.97		-
	26	Fl	-	1.13	66.38	-	-	1.64	-
	28		-	0.31	94.91	-	-	2.97	-
	36		-	0.85	94.22	-	-	2.03	-
	38		-	2.19	76.92	-	-	3.81	-
	26,28,36 And38	ABG	1.1213	107.402	-	12.7045	-		0.25
Urban areas (Uma Scenario)	3.5	Cl	2.15	-	-	-	3.26		-
	28		2.17	-	-	-	3.94		-
Parking lot	28	Cl SPL	2.7	-	-	-	3.7		-
	38	Cl DPL	3.4	-	-	-	3.1		-
		Cl SPL	2.8	-	-	-	1.9		-
		Cl DPL	3.1	-	-	-	3.4		-
	28	Fl SPL	-	3.0	56.8	-	-	3.7	-
		Fl DPL	-	0.8	103	-	-	2.4	-
		Fl SPL	-	2.8	64.6	-	-	1.9	-
	38	Fl DPL	-	0.4	108.5	-	-	1.4	-

Chapter Six

Conclusions and Future Works

6.1 Conclusions

Wireless measurements and simulations campaigns throughout the sub-frequency band at 3.5 GHz were taken for both LOS and NLOS channel conditions at the Electronics Engineering College, Department of Communication Engineering, Ninevah University, Iraq. Path loss of channel modeling was investigated and comparisons were made between simulations using WI ray-tracing software and practical measurements. There was concentration on path loss results for the 3.5 GHz band for indoor corridor channels, but there were also simulation results for the 3.5 and 28 GHz frequency bands for the outdoor environment by using two types of antennas. To assess the good agreement between measurement and simulation campaigns, the commonly used CI, FI for single frequency and ABG for multi frequency path loss models were used. The path loss exponent values differences between simulation and measurement for LOS and NLOS are less than 0.23 and 0.05, respectively. The variations in CI model standard deviation between simulation and measurement are less than 2.9 dB and 2.2 dB For LOS and NLOS scenarios, respectively. In this study, the path loss model slopes were higher than the free space path loss exponent (n=2) value at the NLOS scenario for indoor environment. The difference of CI path loss exponent values at 3.5 and 28GHz for outdoor environment is less than 0.12, 0.46 and 0.58 for horn, omnidirectional and horn-omnidirectional antennas when both antennas are vertically polarized. Whereas when the transmitter antenna is vertical polarization and the receiver is horizontal polarization the difference of the PLEs values are

less than 0.39, 0.57 and 1.32 for horn, omnidirectional and horn-omnidirectional antennas. At both polarizations, the model fit standard deviation values for the 28GHz frequency band are higher than those for the 3.5GHz frequency band. The ABG and CI models are both viable omnidirectional and directional path loss models to evaluate for the outdoor scenario, with the ABG model being similar to the FI model in that it uses offsets. When contrasted to the ABG or FI models, the CI model has a physical relationship to transmitted power and a frequency-dependent path loss factor in the first meter, resulting in PLEs that are significantly more consistent over wide frequency ranges, with about comparable shadowing standard deviation. For each environment, path loss for different models was determined as a function of distance. It can be concluded that the path loss increased with higher frequency in addition to long distances between both antennas.

6.2 Future Works

For future work in this field it is suggested to focus on followings:

1. More measurements for 28 GHz narrowband channel path loss are needed for indoor corridor building and outdoor environments.
2. For mm Wave path loss effects, simulation features, such as the number of propagation paths and antenna patterns need to be fine-tuned. Material parameters and rough-surface scattering parameters can be tweaked to a lesser extent. There is also a need for more precise modeling of floor plans and obstacles.
3. More materials attenuation (penetration loss) research, using both measurement and simulation, should be carried out for real-world building structures with various types of layers and complex composition.

4. Finally, measurements of millimeter wave massive MIMO for 28 GHz and sub-frequency band for 3.5GHz should be made and compared to massive MIMO simulations.

References

[1] H. Viswanathan and M. Weldon, "The Past, Present, and Future of Mobile Communications," Bell Labs Tech. Journal, vol. 19, pp. 8–21, 2014.

[2] D. C. Cox, "Fundamental limitations on increasing data rate in wireless systems," IEEE Communication Magazine, vol. 46, no. 12, pp. 16–17, 2008.

[3] M. Stefanovic, S. R. Panic, R. A. A. De Souza, and J. Reig, "Recent Advances in RF Propagation Modeling for 5G Systems," International Journal Antennas Propagation, 2017.

[4] Y. Yang, J. Xu; G. Shi, and C. X. Wang, "5G Wireless Systems,Simulation and Evaluation,"1st Ed.(Springer International), 2018.

[5] A. Osseiran *et al.*, "Scenarios for 5G mobile and wireless communications: The vision of the METIS project," IEEE Communication Magazine, vol. 52, no. 5, pp. 26–35, 2014.

[6] Nokia White paper, "5G deployment below 6 GHz," pp. 1–12, 2017, [Online]. Available: www.nokia.com.

[7] P.S.M. Tripathi and R.Prasad,"5G Spectrum Services," Wireless Personal Communication, vol.100, no.2, pp.539-555, 2018.

[8] J. Stanley," The State of 5G: When It's Coming, How Fast It Will Be & The Sci-Fi Future It Will Enable", [Online], available: https://www.techspot.com/article/1582-stateof-5g-wireless/page2.

[9] United States Frequency Allocation chart, [Online], Available: https://www.ntia.doc.gov/page/2011/united-states-frequency-allocation-chart.

[10]   J. Liu, "Channel Modeling and Tropospheric Effects on Millimeter Wave Communications for Aviation Applications,", PHD. Dissertation, College of Engineering and Computing, South Carolina University, Colombia, 2020.

[11]   GSMA, "5G Spectrum," Public Policy Position, no. July, 2016, [Online]. Available: https://www.gsma.com/spectrum/wp-content/uploads/2016/06/GSMA-5G-Spectrum-PPP.

[12]   P. Tracy, "5G in the sub-6 GHz spectrum bands", [Online], Available: https://www.rcrwireless.com/20160815/fundamentals/5g-sub-6ghz-tag31-tag99.

[13]   A. Chandra, A. Kumar and P. Chandra," Estimation of Path Loss Parameters Using Propagation Measurements. At 900 MHz and 1.89 GHz in the Corridors of A Multifloor Building," IEEE Communication Magazine, 1998.

[14]   T. Chrysikos, G. Georgopoulos, and S. Kotsopoulos, "Site-specific validation of ITU indoor path loss model at 2.4 GHz," IEEE International Symposium World Wireless, Mob. Multimed. Networks Work. WOWMOM, no. 978, 2009.

[15]   A. Valcarce and J. Zhang, "Empirical Indoor-to-Outdoor Propagation Model for Residential Areas at 0.9–3.5 GHz," IEEE Antennas and Wireless Propagation Letters vol. 9, pp. 682–685, 2010.

[16]   D. W. Matolak and R. Sun, "Air-Ground Channel Characterization for Unmanned Aircraft Systems-Part I: Methods, Measurements, and Models for Over-Water Settings," IEEE Transtion Vehichle Technology, vol. 66, no. 1, pp. 26–44, 2017.

[17]   H. Zheng, W. Li, L. Tian, C. Xu, F. Huang, and J. Zhang, "Path loss models for urban macro cell scenario at 3.35, 4.9 and 5.4 GHz,"

IEEE International Symposium Personal, Indoorand Mobile Radio Communications(PIMRC), pp. 2229–2233, 2015.

[18]   S. Sun, T. A. Thomas, T. S. Rappaport, H. Nguyen, I. Z. Kovacs, and I. Rodriguez, "Path loss, shadow fading, and line-of-sight probability models for 5G urban macro-cellular scenarios," IEEE Global Communications Conference Workshop (Globecom Workshop) , 2015.

[19]   C. H. Chio and S. W. Ting, "Empirical model indoor corridor path loss at 5 GHz," International Sympous Antennas Propagation (ISAP), pp. 206–207, 2017.

[20]   S. Sun et al., "Investigation of Prediction Accuracy, Sensitivity, and Parameter Stability of Large-Scale Propagation Path Loss Models for 5G Wireless Communications," IEEE Transtion Vehicular Technology, vol. 65, no. 5, pp. 2843–2860, 2016.

[21]   A. M. Al-Samman, T. Abd Rahman, and M. H. Azmi, "Indoor corridor wideband radio propagation measurements and channel models for 5G millimeter wave wireless communications at 19 GHz, 28 GHz, and 38 GHz Bands," Wireless Communication Mobile Computer, pp. 1-12,2018.

[22]   H. A. Obeidat,R.Asit;N.T.Ali,Y.A.Dama, et al., "An Indoor Path Loss Prediction Model Using Wall Correction Factors for Wireless Local Area Network and 5G Indoor Networks," in Radio Science, vol. 53, no. 4, pp. 544–564, 2018.

[23]   H. K. Hoomod, I. Al-Mejibli, and A. I. Jabboory, "Analyzing Study of Path loss Propagation Models in Wireless Communications at 0.8 GHz," Journal Physical Conference Series, vol. 1003, no. 1, pp. 0–8, 2018.

[24] K. Szczypiorski, A. Janicki, and S. Wendzel, "'The good, the bad and the ugly': Evaluation of Wi-Fi steganography," Journal Communication, vol. 10, no. 10, pp. 747–752, 2015.

[25] J. Liu, D. W. Matolak, M. Mohsen, and J. Chen, "Path loss modeling and ray-tracing verification for 5/31/90 GHz indoor channels," IEEE Vehicular Technology Conference, pp. 1–6, 2019.

[26] M. Sameer, KH. H.Sayidmarie, A. Aboud,"Investigation of indoor propagation of WLAN signals," Indonesian Journal of Electrical Engineering and Computer Science, 2019.

[27] F. Hossain, T.Kim.Th.Abd Rahman et al., "Indoor 3-D RT radio wave propagation prediction method: PL and RSSI modeling validation by measurement at 4.5 GHz," Journal of Electronics, vol. 8, no. 7, 2019.

[28] M. Schmieder, T. Eichler, S. Wittig, M. Peter, and W. Keusgen, "Measurement and characterization of an indoor industrial environment at 3.7 and 28 GHz," 14th European Conference on Antennas and Propagation (EuCAP), Copenhagen, Denmark, pp. 2–6, 2020.

[29] Y. Guan, J. Zhang, L. Tian, P. Tang, and T. Jiang, "A Comparative Study for Indoor Factory Environments at 4.9 and 28 GHz," 14th European Conference Antennas and Propagation, (EuCAP), no. 92, pp. 8–12, 2020.

[30] K. S. Muttair, O. A. Shareef, and M. F. Mosleh, "Outdoor to Indoor Wireless Propagation Simulation Model for 5G Band Frequencies," IOP Conference Series Material Science Engineering, vol. 745, no. 1, 2020.

[31]   M. Dohler et al., "The 5G wireless propagation channel models," 5G Mobile Wireless Communication Technology," pp. 357–380, 2016.

[32] J. Zander, B. Slimane, and L. Ahlin," Principles of Wireless Communications," 1st Ed. (Eurographic Lund), 2018.

[33] N.Muthukumaran and R.Sonya," Principles of Wireless Communications," 1st Ed. pp.68-70,(Scholars' Press), 2017.

[34] Rappaport, "Wireless communication,"1st Ed. vol. 28, no. 7. pp. 310, (IBM technical disclosure bulletin),2011.

[35]   Christopher Haslett," Essentials of Radio Wave Propagation," 1st Ed. (William Webb Ofcom), UK, 2008.

[36]   L. Azpilicueta, M. Rawat, K. Rawat, F. Ghannouchi, and F. Falcone, "Convergence analysis in deterministic 3D ray launching radio channel estimation in complex environments," Application Computer Electromagnetic Soc. Journal, vol. 29, no. 4, pp. 256–271, 2014.

[37]   M. Khatun, H. Mehrpouyan, and D. Matolak, "60-GHz millimeter-wave pathloss measurements in boise airport," IEEE/AIAA 36th Digital Avionics Systems Conference (DASC), St. Petersburg, FL, pp. 1276–1280, 2017.

[38] Alexander L. Grant," Path Loss Models for Two Small Airport Indoor Environments at 31 GHz", MSc. Dissertation, Department of Engineering and Computing, South Carolina University, Colombia, 2019.

[39]   R. Zabihi and R. Vaughan, "Diffraction: A critical propagation mechanism," Can. Conference Electronics Computer Engineering, no. 3, pp. 3–6, 2016.

[40] S. Rangan, T. S. Rappaport, and E. Erkip, "Millimeter-wave cellular wireless networks: Potentials and challenges," Proceding IEEE, vol. 102, no. 3, pp. 366–385, 2014.

[41] A. F. Molisch, "Wireless Communications", 2nd Ed. (IEEE Press - Wiley), 2011.

[42] A. Ghasemi, A. Abedi, and F. Ghasemi," Propagation engineering in wireless communications", 2nd Ed.(Springer International Publishing Switzerland) 2016.

[43]　J. S. Seybold, "Introduction to RF Propagation".1st Ed.(John Wiley & Sons, Inc.),2005.

[44] T. Bakth," Analysis for frequencies for future 5G system by positioning receiver at different altitudes," MSc. Dissertation, Department of Electrical Engineering, Mathematics and Science, 2020.

[45] G. R. Maccartney, T. S. Rappaport, S. Sun, and S. Deng, " Indoor office wideband millimeter-wave propagation measurements and channel models at 28 and 73 GHz for ultra-dense 5G wireless networks," IEEE Access, vol. 3, pp. 2388–2424, 2015.

[46] G. R. MacCartney Jr.,Shu Sun, et al." Millimeter wave wireless communications: New results for rural connectivity," in All Things Cellular16, in conjunction with ACM (Mobile Communication), 2016.

[47] I. S. Batalha et al." Indoor corridor office propagation measurements and channel models at 8, 9, 10 and 11 GHz" IEEE Access, vol. 7, pp. 55 005– 55 021, 2019.

[48] L. Rubio, Rafael P. et al." Contribution to the Channel Path Loss and Time-Dispersion Characterization in an Office Environment at 26 GHz".Journal of Electronics, 8, 1261, 2019.

[49] D. Pimienta, D. Valle et al.," Indoor Path Loss Measurements at the 5G Millimeter-Wave Bands of 26 and 39 GHz," 13th European Conference on Antennas and Propagation (EuCAP), pp. 1–5, 2019.

[50] T. S. Rappaport et al., " Wideband millimeter-wave propagation measurements and channel models for future wireless communication system design," IEEE Transtion Common, vol. 63, no. 9, pp. 3029–3056, 2015.

[51] H. Munir, S. A. Hassan; H. Pervaiz, Q. Ni and L. Musavian," Resource optimization in multi-tier HetNets exploiting multi-slope path loss model,'' IEEE Access, vol. 5, pp. 8714–8726, 2017.

[52] H. Wang, P. Zhang, J. Li and X. You, " Radio propagation and wireless coverage of LSAA-based 5G millimeter-wave mobile communication systems," China Communication, vol. 16, no. 5, pp. 1–18, 2019.

[53] X. Cai,A.Gonzalez;D.Aloonso et al.," Low altitude UAV propagation channel modeling," in Proc. 11th Europe Conference Antennas Propagation, (EuCAP), France, pp. 1443–1447, 2017.

[54] Th. Chrysikos, P. Georgakopoulos et al." Measurement-based characterization of the 3.5 GHz channel for 5G-enabled IoT at complex industrial and office topologies," Wireless Telecommunications Symposium (WTS), Phoenix, AZ, pp. 1-9, 2018.

[55] A. Sulyman, , A. Alwarafy, G. MacCartney, T. Rappaport and A. Alsanie, " Directional radio propagation path loss models for millimeter-wave wireless networks in the 28-, 60-, and 73-GHz bands," IEEE Transition Wireless Communication, vol. 15, no. 10, pp. 6939–6947, 2016.

[56] D. Alam and R. Huque," Comparative Study of Path Loss Models of WiMAX at 2.5 GHz Frequency Band," International Journal of Future Generation Communication and Networking, vol. 6, no. 2, 2013.

[57] V. S. Abhayawardhana, I. J. Wassell, D. Crosby, M. P. Sellars and M. G. Brown," Comparison of empirical propagation path loss models for fixed wireless access systems,'' in Proc. IEEE 61st Vehicular Technology Conference, vol. 1, pp. 73–77, 2005.

[58] Purnima.K.Sharma and R.K.Singh." Comparative Analysis of Propagation Path loss Models with Field Measured Data," International Journal of Engineering Science and Technology vol. 2(6), 2013.

[59] S. Sun, G. R. MacCartney, Jr and T. S. Rappaport," Millimeter-wave distance dependent large-scale propagation measurements and path loss models for outdoor and indoor 5G systems," in Proc. 10th Europe Conference Antennas Propagation (EuCAP), pp. 1–5, 2016.

[60] T. S. Rappaport et al., "Overview of millimeter wave communications for fifth-generation (5G) wireless networks—With a focus on propagation models," IEEE Transition Antennas Propagation, vol. 65, no. 12, pp. 6213–6230, 2017.

[61] N. O. Oyie and T. J. O. Afullo. " A Comparative study of dual-slope path loss model in various indoor environments at 14 to 22 GHz," Progress in Electromagnetics Research Symposium (PIERS-Toyama), pp.121-128, 2018.

[62] A. Bhuvaneshwari, R.Hemalatha , T. Satyasavithri." Path loss prediction analysis by ray tracing approach for NLOS indoor propagation," International Conference on Signal Processing and Communication Engineering Systems, 2015.

[63] N.Hewa, S. Kandeepan, M. Ding, A. Al-Hourani and K. M. Gomez," Diversity based coverage improvement for air-to-ground wireless channels," IEEE International Conference on Wireless for Space and Extreme Environments (WiSEE), 2019.

[64] D. Guillaume,A.Alayon and B. Allen." LTE-Advanced and Next Generation Wireless Networks: Channel Modeling and Propagation," 1st Ed. (A John Wiley & Sons, Ltd.), 2013.

[65] "Wireless InSite, Reference Manual, Version 2.6.3, REMCOM Inc., 315 S. Allen St., Suite 416 State College, PA 16801, 2011.

[66] M. Kacou, V. Guillet, G. E. Zein and G. Zaharia, "A multi-wall and multi-frequency home environment path loss characterization and modeling," 12th European Conference on Antennas and Propagation (EuCAP 2018), London, UK , pp. 1-5, 2018.

[67] H. Zheng, W. Li, L. Tian and C. Xu, et al., "Path loss models for urban macro cell scenario at 3.35, 4.9 and 5.4 GHz," IEEE 26th Annual International Symposium on Personal, Indoor, and Mobile Radio Communications (PIMRC), China, , pp. 2229-2233, 2015.

[68] N. Mehrnia and M.Kemal. " Ray tracing-based maritime channel analysis for millimeter radio waves," Journal of Infrared, Millimeter, and Terahertz Waves 40.1: pp.108-130, 2019.

[69] T. Rama, D. Balachander and N. Tiwari, "Short-range near floor path gain measurements in indoor corridors at UHF for wireless sensor communications," IEEE International Conference on Communication Systems (ICCS), Singapore, pp. 189-193, 2012.

[70] M. N. Hindia, A. M. Al-Samman, T. A. Rahman, and T. M. Yazdani, "Outdoor large-scale path loss characterization in an urban environment at 26, 28, 36, and 38 GHz," Journal of Physical Communication, vol. 27, pp. 150–160, 2018.

[71] K. Zhang, R. Zhang, J. Wu, Y. Jiang and X. Tang, "Measurement and Modeling of Path Loss and Channel Capacity Analysis for 5G UMa Scenario," 11th International Conference on Wireless Communications and Signal Processing (WCSP) , pp. 1-5, 2019.

[72] A.M. Al-Samman, T. Abd Rahman, M. N. Hindia , A. Daho and E. Hanaf," Path loss model for outdoor parking environments at 28 GHz and 38 GHz for 5G wireless networks", journal of symmetry, 10, 672, 2018.

Published Papers

[1] S Kh Al-Khero and Y M Abbosh ,"Path Loss and Channel Modeling at 3.5GHz for 5G Cellular System", The 1st International Ninevah Conference on Engineering and Technology (INCET 2021), (5-6) April 2021, Ninevah University, Mosul, Iraq.

الخلاصة

الجيل الخامس من انظمة الاتصالات الخلوية سيكون الاسرع والاكثر اماناً والاسهل من ناحية الاتصال من شبكات الاتصالات اللاسلكية الحالية .كذلك لتلبية الزيادة في خدمة الاتصالات اللاسلكية بمقدار ألف مرة في السنوات القليلة القادمة, فإن الجيل الخامس قادر على تحسين الشبكة اللاسلكية في ثلاث اتجاهات وهي: زيادة استخدام الطيف الترددي , تحسين تعدد الارسال المكاني وكذلك زيادة عرض النطاق الترددي. من اهم ميزات الجيل الخامس هي استخدام الطيف الترددي الواسع, حيث يعد استخدام الترددات الآقل من 6جيجاهرتز والآعلى منها من بين الموضوعات الاكثرُ بحثاً في أنظمة الأتصالات اللاسلكية.

من اجل تصميم النظام الخلوي اللاسلكي للجيل الخامس وتحليل التغطية للشبكة , فإن من المهم المعرفة الأساسية بخصائص انتشار القناة وعلى وجه الخصوص خاصية فقدان المسار في البيئات الداخلية والخارجية.

في هذه الرسالة ,تم التقصي عن خسارة المسار لنظام الجيل الخامس, حيث تم إجراء القياسات العملية وكذلك المحاكاة عن طريق برنامج(Wireless InSite)عند تردد 3.5 جيجا هرتز في مبنى قسم هندسة الاتصالات جامعة نينوى ,العراق . تم العمل في الطابق الثاني للمبنى بما في ذلك الممر بالنسبة للبيئة الداخلية. حيث تم اخذ حالتين من شروط القناة وهما قناة خط الرؤية وقناة عدم خط الرؤية بالنسبة لكلا الطريقتين العملية والمحاكاة ومقارنتها مع نماذج مختلفة من خسارة المسار بالنسبة للبيئة الداخلية. أظهرت النتائج في حالة قناة خط الرؤية للإشارة عند تردد 3.5جيجاهرتز اقل توهيناً من ما هي عليه في حالة خط عدم الرؤية, حيث ان كلتا الحالتين تتاثران بالعناصر الداخلية .كذلك تم القيام بإجراء عمليات المحاكاة في البيئة الخارجية للمبنى عند نوعين من الترددات للمقارنة بينهما ومقارنتها مع نماذج مختلفة من خسارة المسار. حيث تم حسابها باستخدام برامج Matlab and Excell. أظهرت النتائج إن قيمة أُس فقدان المسار يساوي تقريباً أُس فقدان المسار الحر التي تبلغ قيمتها اثنين بالنسبة لبيئة الانتشار الداخلية , بينما كانت قيمتها اكبر من قيمة أُس فقدان المسار الحر بالنسبة لبيئة الانتشار الخارجية.بالنسبة الى الانحرافات المعيارية للنماذج تناسبت بشكل اكبر مقارنة من تلك الموجودة في البيئات الخارجية.

إقرار لجنة المناقشة

نشهد نحن اعضاء لجنة التقويم و المناقشة باننا قد اطلعنا على هذه الرسالة الموسومة (دراسة خسارة المسارلقناة الجيل الخامس) وناقشنا الطالبة (سيماء خالد نافع الخيرو) في محتوياتها وفيما له علاقة بها بتاريخ   / / 2021 وقد وجدناها جديرة بنيل شهادة الماجستير–علوم في اختصاص هندسة الاتصالات.

التوقيع: التوقيع:

رئيس اللجنة: عضو اللجنة:

التاريخ: التاريخ:

التوقيع: التوقيع:

عضو اللجنة: عضو اللجنة:

التاريخ: التاريخ:

قرار مجلس الكلية

اجتمع مجلس كلية هندسة الالكترونيات بجلسته................... المنعقدة بتاريخ وقرر المجلس منح الطالب شهادة الماجستير–علوم في اختصاص هندسة الاتصالات.

التوقيع: التوقيع:

مقرر المجلس: رئيس مجلس الكلية:

التاريخ: التاريخ:

إقرار المشرف

أشهد بأن هذه الرسالة الموسومة (دراسة خسارة المسارلقناة الجيل الخامس) قد تم اعدادها من قبل الطالبة (سيماء خالد نافع الخيرو) تحت اشرافي في قسم هندسة الاتصالات/ كلية هندسة الالكترونيات / جامعة نينوى, كجزء من متطلبات نيل شهادة الماجستير –علوم في اختصاص هندسة الاتصالات.

التوقيع:

الاسم :أ.م.د.يونس محمود عبوش

التاريخ:

إقرار المقوم اللغوي

أشهد بانه قد تمت مراجعة هذه الرسالة من الناحية اللغوية وتصحيح ما ورد فيها من اخطاء لغوية وتعبيرية وبذلك أصبحت الرسالة مؤهلة للمناقشة بقدر تعلق الامر بسلامة الاسلوب او صحة التعبير .

التوقيع:

الاسم:

التاريخ:

إقرار رئيس قسم هندسة الاتصالات

بناءاً على التوصيات المقدمة من قبل المشرف والمقيم اللغوي ارشح هذه الرسالة للمناقشة.

التوقيع:

الاسم:أ .م.د.يونس محمود عبوش

التاريخ:

إقرار رئيس لجنة الدراسات العليا

بناءاً على التوصيات المقدمة من قبل المشرف والمقيم اللغوي ورئيس قسم هندسة الاتصالات أرشح هذه الرسالة للمناقشة.

التوقيع:

الاسم: أ.م.د.يونس محمود عبوش

التاريخ:

بسم الله الرحمن الرحيم

۞ قُلْ هَلْ يَسْتَوِى ٱلَّذِينَ يَعْلَمُونَ وَٱلَّذِينَ لَا

يَعْلَمُونَ إِنَّمَا يَتَذَكَّرُ أُوْلُواْ ٱلْأَلْبَـٰبِ ۞

صدق الله العظيم

دراسة خسارة المسار لقناة الجيل الخامس

دراسة تقدمت بها

سيماء خالد نافع الخيرو

الى

مجلس كلية هندسة الالكترونيات

جامعة نينوى

كجزء من متطلبات نيل شهادة الماجستير

في هندسة الاتصالات

باشراف

الاستاذ المساعد الدكتور يونس محمود عبوش

1442هـ	**2021م**

وزارة التعليم العالي والبحث العلمي

جامعة نينوى

كلية هندسة الالكترونيات

قسم هندسة الاتصالات

دراسة خسارة المسار لقناة الجيل الخامس

سيماء خالد نافع الخيرو

رسالة ماجستير

علوم في

هندسة الاتصالات

باشراف

الاستاذ المساعد الدكتور يونس محمود عبوش

1442هـ   2021م